OMEG
Origin of Matter and Evolution of Galaxies
Key Research Institutes in Universities

The first University in Korea
Soongsil University

# Neutrino-process in Core-collapsing supernova explosion (CCSN)


**Myung-Ki Cheoun**
(Soongsil University, OMEG Institute, Seoul, Korea)


In collaboration with


Heamin Ko,[1] Myung-Ki Cheoun [a],[1] Eunja Ha,[1] Motohiko Kusakabe,[2] Takehito Hayakawa,[3] Hirokazu Sasaki,[4] Toshitaka Kajino,[2,4] M. Hashimoto,[5] M. Ono,[6] M. D. Usang,[7] S. Chiba,[7] K. Nakamura,[8] A. Tolstov,[9] K. Nomoto,[9] T. Kawano,[10] and G. J. Mathews[11]


PRL 121, 102701 (2018), Acta Phys. Pol. B, 50, 385(2019),
ApJL 891, L24 (2020), ApJ 894, 1 (2020), ApJ in press (2022) …

**TRIUMF-APCTP Joint Workshop, Aug. 8-12, 20222**

# Contents

- **Motivation**
- **Neutrino Process in Supernova Explosion**

- **Neutrino Oscillation in vacuum and matter, and neutrino Self-Interaction in the Neutrino Process**
- **Neutrino-induced Reactions by QRPA**
- **Dependence on Neutrino Luminosity**

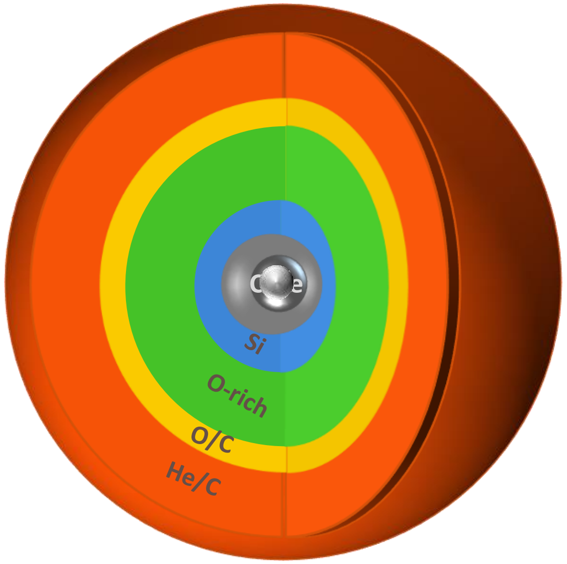


- **Heavy Elements ($^{92}$Nb, $^{98}$Tc, $^{138}$La, $^{180}$Ta ...)**
- **Light Elements ($^{7}$Li, $^{11}$Be...) & Ratios of $^{7}$Li/$^{11}$B and $^{138}$La/$^{11}$B**

- **Cosmological origin of $^{10}$Be**

- **Sterile Neutrinos & Shock Effects in Neutrino Process**

- **Summary**

# Periodic Table and Origins of Elements

## Periodic Table

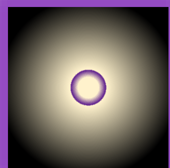

Bing Bang

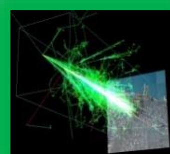

Cosmic Rays

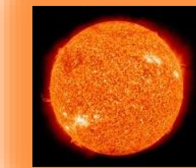

Dying Small Stars

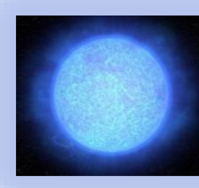

Exploding Massive Stars

Supernova & NS merge

| | | | | | | | | | | | | | | | | | |
|---|---|---|---|---|---|---|---|---|---|---|---|---|---|---|---|---|---|
| H | | | | | | | | | | | | | | | | | He |
| Li | Be | | | | | | | | | | | B | C | N | O | F | Ne |
| Na | Mg | | | | | | | | | | | Al | Si | P | S | Cl | Ar |
| K | Ca | Sc | Ti | V | Cr | Mn | Fe | Co | Ni | Cu | Zn | Ga | Ge | As | Se | Br | Kr |
| Rb | Sr | Y | Zr | Nb | Mo | Tc | Ru | Rh | Pd | Ag | Cd | In | Sn | Sb | Te | I | Xe |
| Cs | Ba | | Hf | Ta | W | Re | Os | Ir | Pt | Au | Hg | Tl | Pb | Bi | Po | At | Rn |
| Fr | Ra | | Rf | Db | Sg | Bh | Hs | Mt | Ds | Rg | Cn | Nh | Fl | Mc | Lv | Ts | Og |
| | | | La | Ce | Pr | Nd | Pm | Sm | Eu | Gd | Tb | Dy | Ho | Er | Tm | Yb | Lu |
| | | | Ac | Th | Pa | U | Np | Pu | Am | Cm | Bk | Cf | Es | Fm | Md | No | Lr |

# Preliminary Evolution of Element Abundances in the Universe Evolution

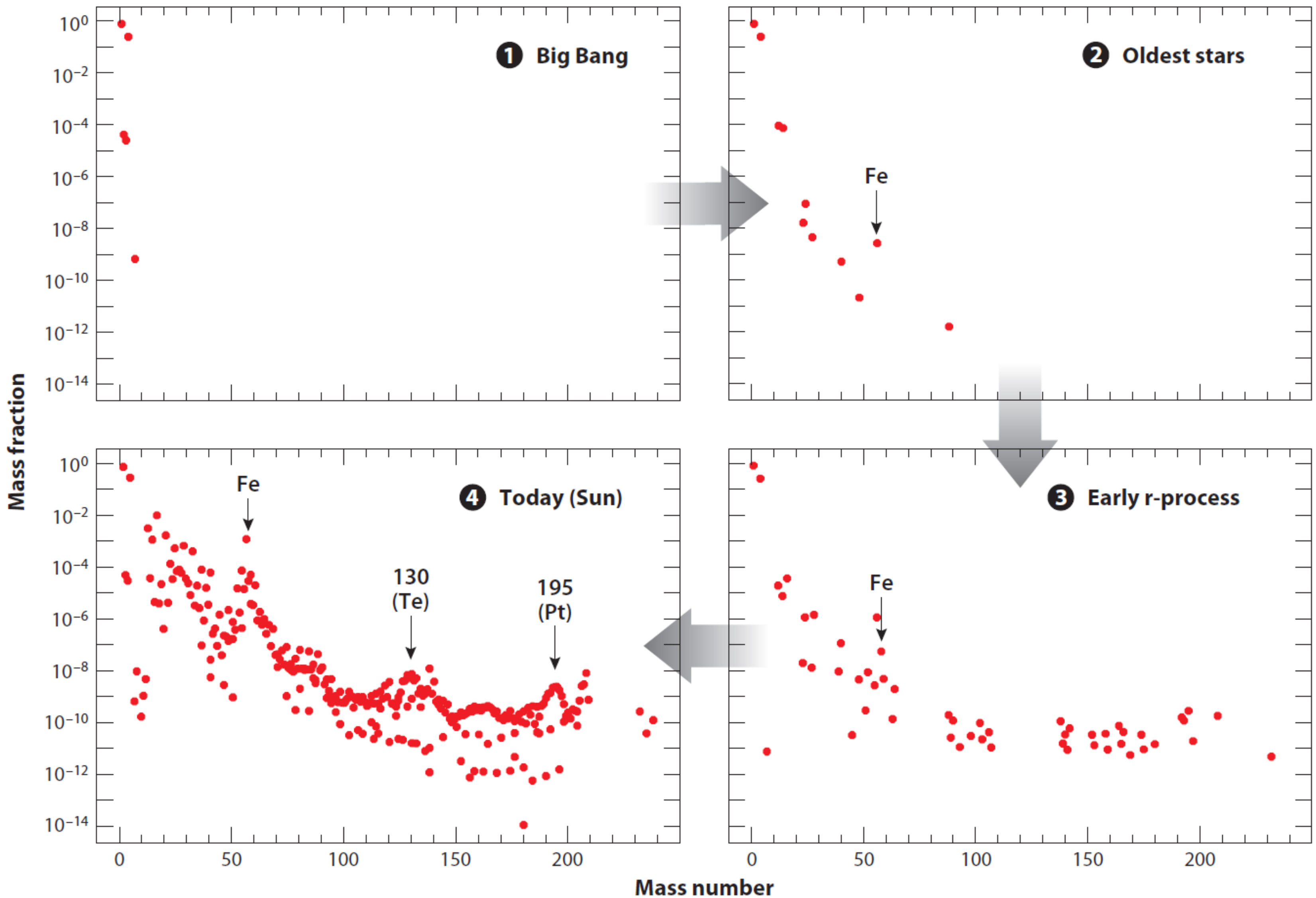


M. Wiescher et al., Annu. Rev. Astro. Astrophys. (2012)

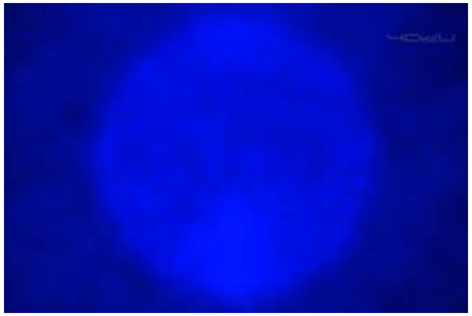

## r-process in SN

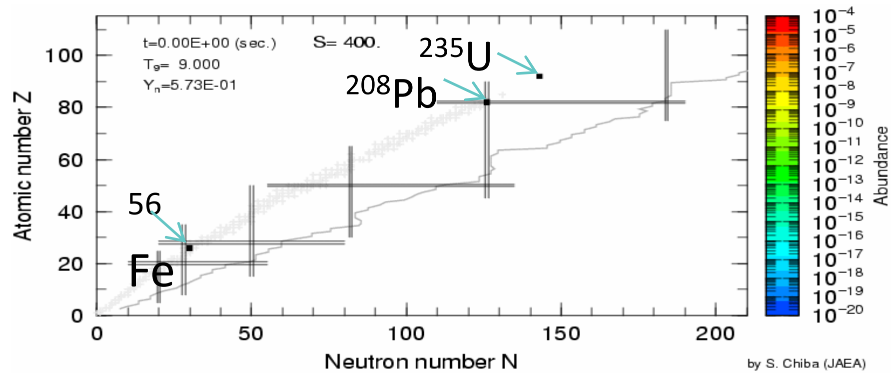


PHYSICAL REVIEW LETTERS 121, 102701 (2018)

H. Ko, M.K. Cheoun et al.

**Short-Lived Radioisotope $^{98}$Tc Synthesized by the Supernova Neutrino Process**

## A Supernova Secret May Be Hidden Inside Meteorites

By Bill Andrews | September 4, 2018 3:50 pm

Discover SCIENCE FOR THE CURIOUS

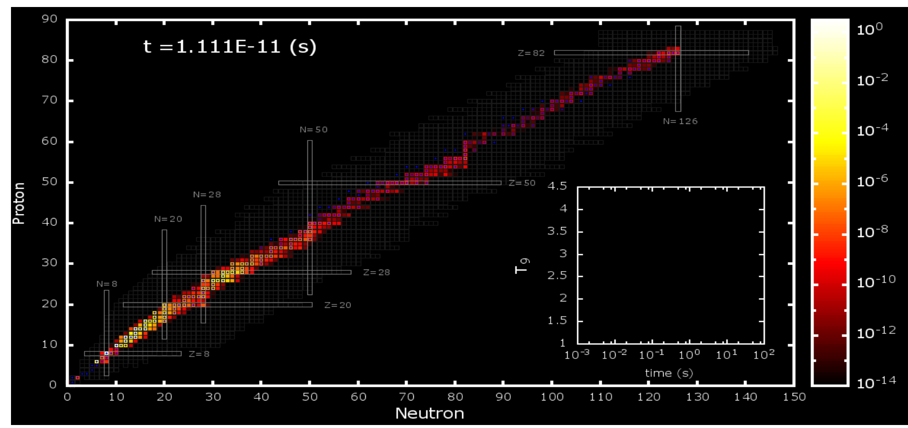


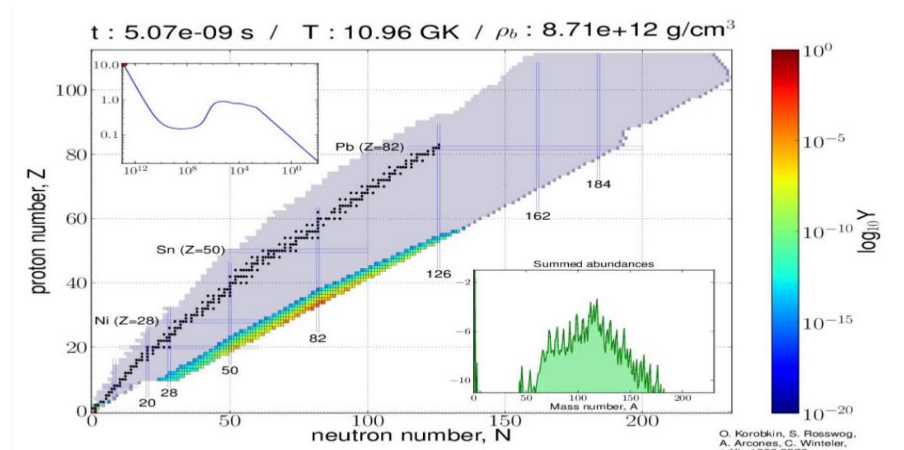


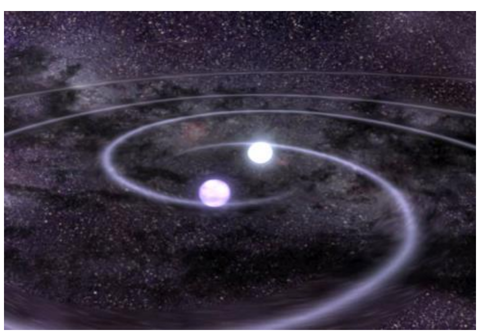

## Nucleosynthesis in Neutron Star Merge

# Contents

- **Motivation**
- **Neutrino Process in Supernova Explosion**
- Neutrino Oscillation in vacuum and matter, and neutrino Self-Interaction in the Neutrino Process
- Neutrino-induced Reactions by QRPA
- Dependence on Neutrino Luminosity
- Heavy Elements ($^{92}$Nb,$^{98}$Tc,$^{138}$La,$^{180}$Ta ...)
- Light Elements ($^{7}$Li,$^{11}$Be...) & Ratio of $^{11}$B/$^{138}$La
- Cosmological origin of $^{10}$Be
- Sterile Neutrinos & Shock Effects in Neutrino Process
- Summary

## Why neutrino process in SN?

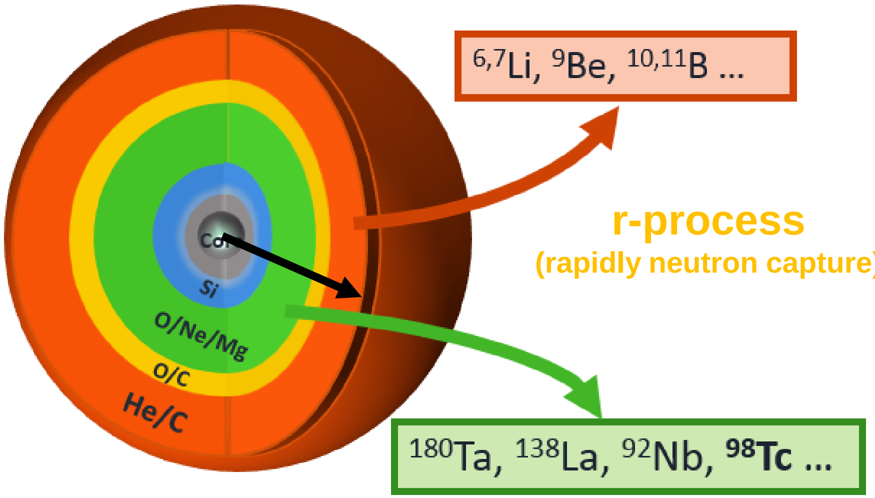


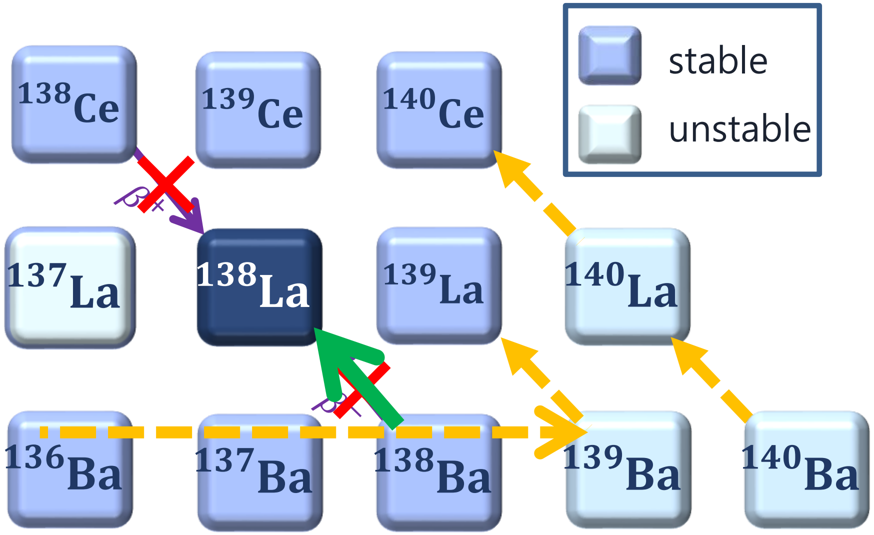


$^{138}\text{Ba}(\nu_e, e^-)^{138}\text{La}$

The first University in Korea
Soongsil University

# Contents

- **Motivation**
- **Neutrino Process in Supernova Explosion**
- **Neutrino Oscillation in vacuum and matter, and neutrino Self-Interaction in the Neutrino Process**
- **Neutrino-induced Reactions by QRPA**
- **Dependence on Neutrino Luminosity**
- **Heavy Elements ($^{92}$Nb, $^{98}$Tc, $^{138}$La, $^{180}$Ta ...)**
- **Light Elements ($^{7}$Li, $^{11}$Be...) & Ratio of $^{11}$B/$^{138}$La**
- **Cosmological origin of $^{10}$Be**
- **Sterile Neutrinos & Shock Effects in Neutrino Process**
- **Summary**

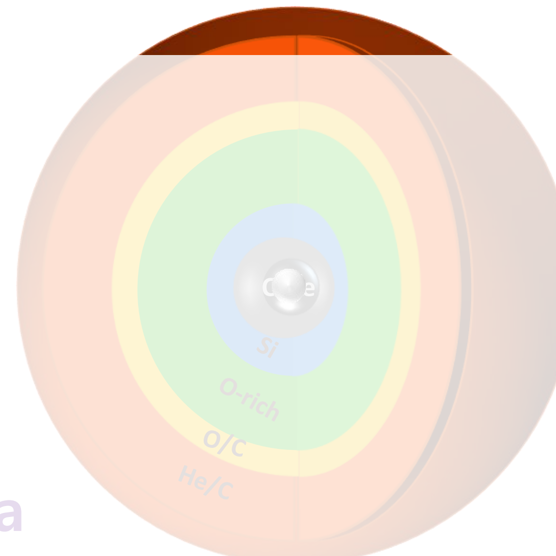

## Total Hamiltonian for neutrino propagation in matter

$$H_{\text{total}} = H_{\text{Vacuum}} + V_{\text{matter}} + V_{\text{self}}$$

### - Vacuum and matter term

$$H_{\text{Vacuum}} = \frac{1}{2\epsilon_\nu} U \begin{pmatrix} 0 & 0 & 0 \\ 0 & \Delta m_{21}^2 & 0 \\ 0 & 0 & \Delta m_{31}^2 \end{pmatrix} U^\dagger, \qquad V_{\text{matter}}(r, E, \theta_p) = \begin{pmatrix} \pm\sqrt{2} G_F n_e & 0 & 0 \\ 0 & 0 & 0 \\ 0 & 0 & 0 \end{pmatrix}$$

Unitary mixing PMNS matrix

$$U = \begin{pmatrix} c_{12}c_{13} & s_{12}c_{13} & s_{13} \\ -s_{12}c_{23} - c_{12}s_{23}s_{13} & c_{12}c_{23} - s_{12}s_{23}s_{13} & s_{23}c_{13} \\ s_{12}s_{23} - c_{12}c_{23}s_{13} & -c_{12}s_{23} - s_{12}c_{23}s_{13} & c_{23}c_{13} \end{pmatrix}$$

Neutrino parameters

$\theta_{12} = 33.8°, \theta_{23} = 45°, \theta_{13} = 9.2°$

$\Delta m_{21}^2 = 7.54 \times 10^{-5}$ [eV$^2$], $|\Delta m_{31}^2| \approx 2.4 \times 10^{-3}$ [eV$^2$]

K. A. Olive, *et al*. [Particle Data Group], Chin. Phys. C 38, 090001 (2014).

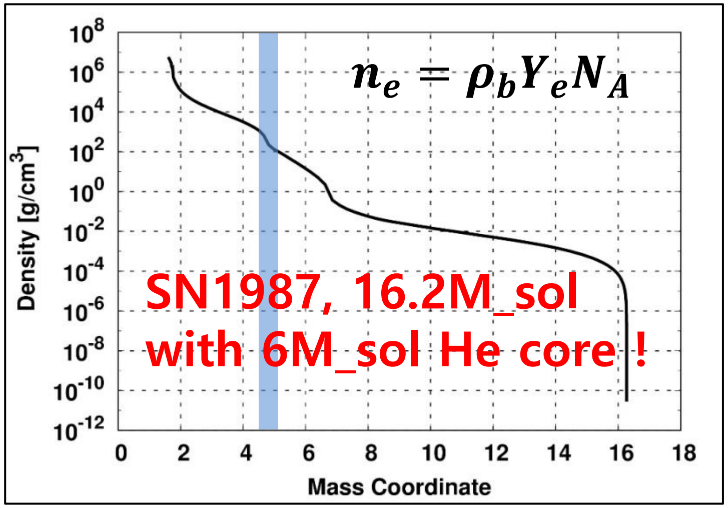


A. Tolstov, in private communication (2017)

### - Neutrino self-interaction term

$$V_{\text{self}}(r, E, \theta_p) = \sqrt{2} G_F \sum_\alpha \left[ \int (1 - \hat{p} \cdot \hat{q})\, \rho_{\nu_\alpha}(q) dn_{\nu_\alpha} dq - \int (1 - \hat{p} \cdot \hat{q})\, \rho^*_{\bar{\nu}_\alpha}(q) dn_{\bar{\nu}_\alpha} dq \right]$$

$$= \frac{\sqrt{2} G_F}{2\pi R_\nu^2} \sum_\alpha \left[ \int dE\, d(\cos\theta_q)(1 - \cos\theta_p \cos\theta_q) \left\{ \frac{L_{\nu_\alpha}}{\langle \epsilon_{\nu_\alpha} \rangle} f_{\nu_\alpha}(E) \rho - \frac{L_{\bar{\nu}_\alpha}}{\langle \epsilon_\nu \rangle} f_{\bar{\nu}_\alpha}(E) \bar{\rho} \right\} \right]$$

**H. Sasaki, *et al.*, Phys. Rev. D 96, 043013 (2017)**

**Heamin KO, et.al, ApJS (2022)**

# Self-Interaction effects on the **Neutrino Flux**


$H_{\text{Vacuum}} + V_{\text{matter}} + V_{\text{self}}$

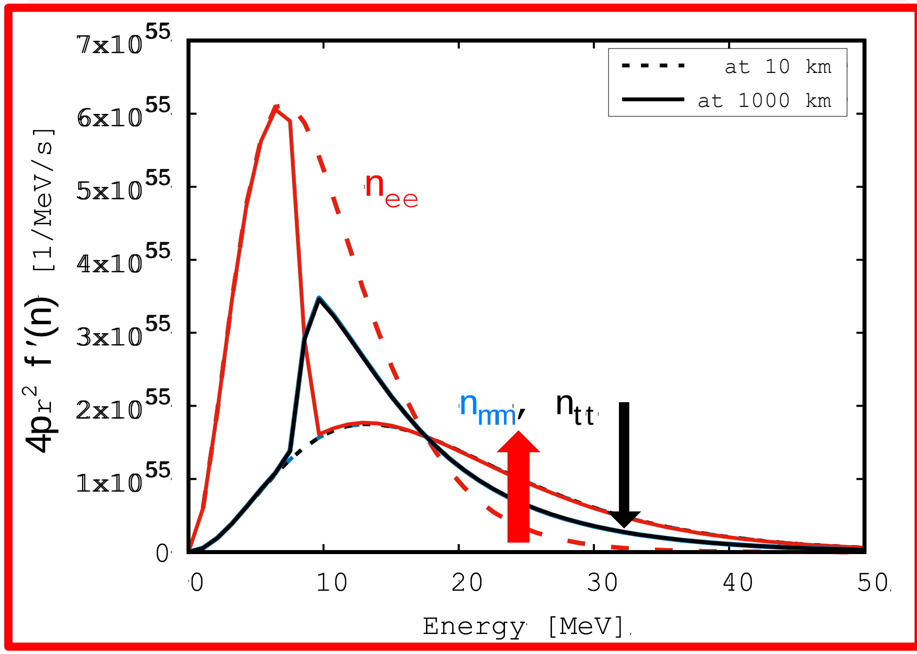


H. Sasaki, *et al.*(NAOJ) in private communication (2018)

**Inverted mass hierarchy (IH)**

The differential neutrino flux with neutrino flavor $\alpha$

$$\phi'(t,r;\epsilon_\nu,T_\alpha) \equiv \frac{d}{d\epsilon_\nu}\phi(t,r;\epsilon_\nu,T_\alpha)$$

$$= \frac{L_\nu}{4\pi r^2}\frac{1}{\langle\epsilon_\nu\rangle}\frac{\epsilon_\nu^2}{\exp(\epsilon_\nu/T_\alpha)+1}\langle\rho_{\alpha\alpha}\rangle$$

The neutrino temperatures are

$$T_{\nu_e} = 3.2,\ T_{\bar{\nu}_e} = 5 \text{ and } T_{\nu_x} = 6\ [\mathrm{MeV}/k_B]$$

T. Yoshida, *et al.*, Astrophys. J. 686, 448 (2008)

- ✓ Initially we assume Fermi-Dirac distribution for neutrino spectra (Case I).
- ✓ In the case of normal mass hierarchy, the SI effect is suppressed.
- ✓ For anti-neutrino, similar effects are found.
- ✓ **We extend it by using other numerical luminosity by the neutrino transport simulation.**

# Neutrino process MSW Effects on the **Neutrino Flux (IH)**

$$\rho_{res} = \frac{\cos 2\theta_{ij}|\Delta m^2_{ji}|}{2\sqrt{2}G_F Y_e E_\nu N_A}.$$

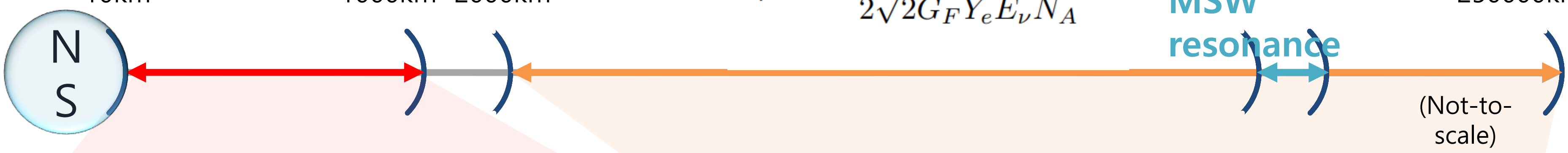


$H_{\text{Vacuum}} + V_{\text{matter}} + V_{\text{self}}$

$H_{\text{Vacuum}} + V_{\text{matter}}$ ( MSW effect)

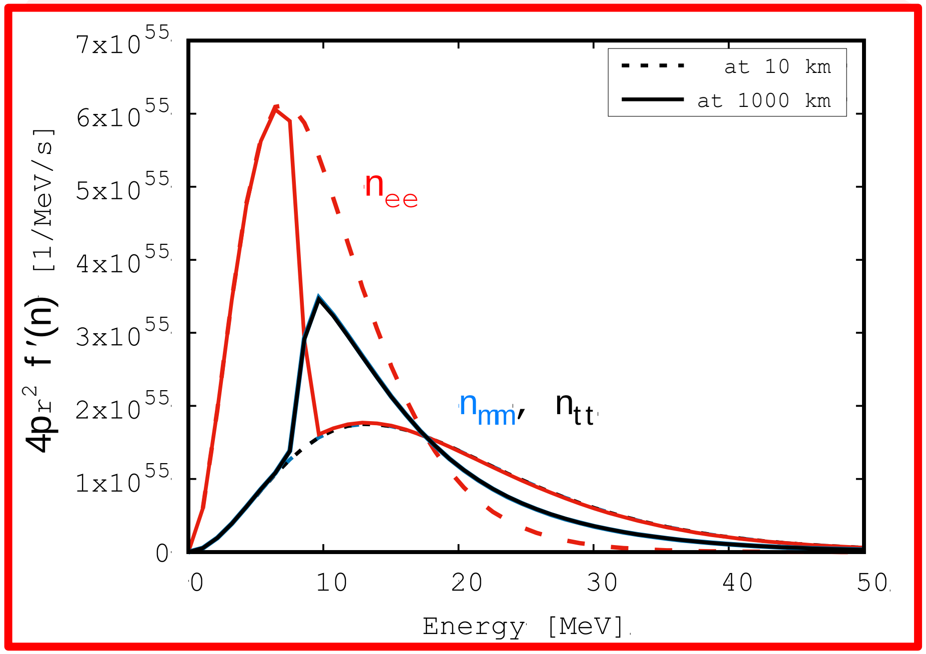


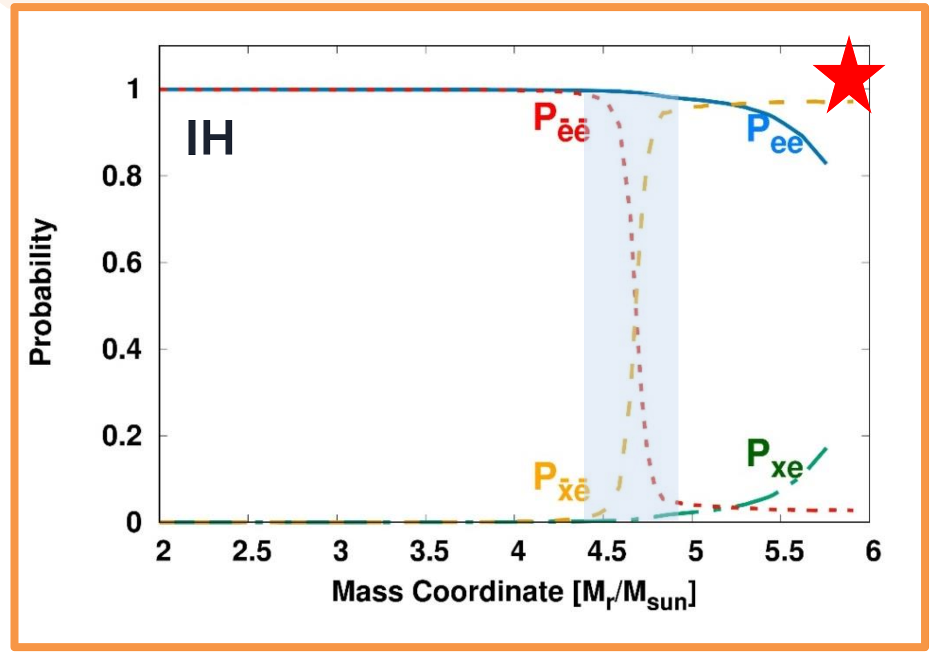


H. Sasaki, *et al.*(NAOJ) in private communication (2018)

The differential neutrino flux **again** including outer region oscillation

$$\frac{d}{d\epsilon_\nu}\phi_\alpha(t,r;\epsilon_\nu,T_\alpha) = \frac{L_\nu(t)}{4\pi r^2}\frac{1}{\langle\epsilon_\nu\rangle}\frac{\epsilon_\nu^2}{\exp(\epsilon_\nu/T_\alpha)+1}\langle\rho_{\alpha\alpha}(t)\rangle \times P_{\alpha\beta}(\epsilon_\nu)$$

$$\rho_{res} = \frac{\cos 2\theta_{ij} |\Delta m^2_{ji}|}{2\sqrt{2} G_F Y_e E_\nu N_A}.$$

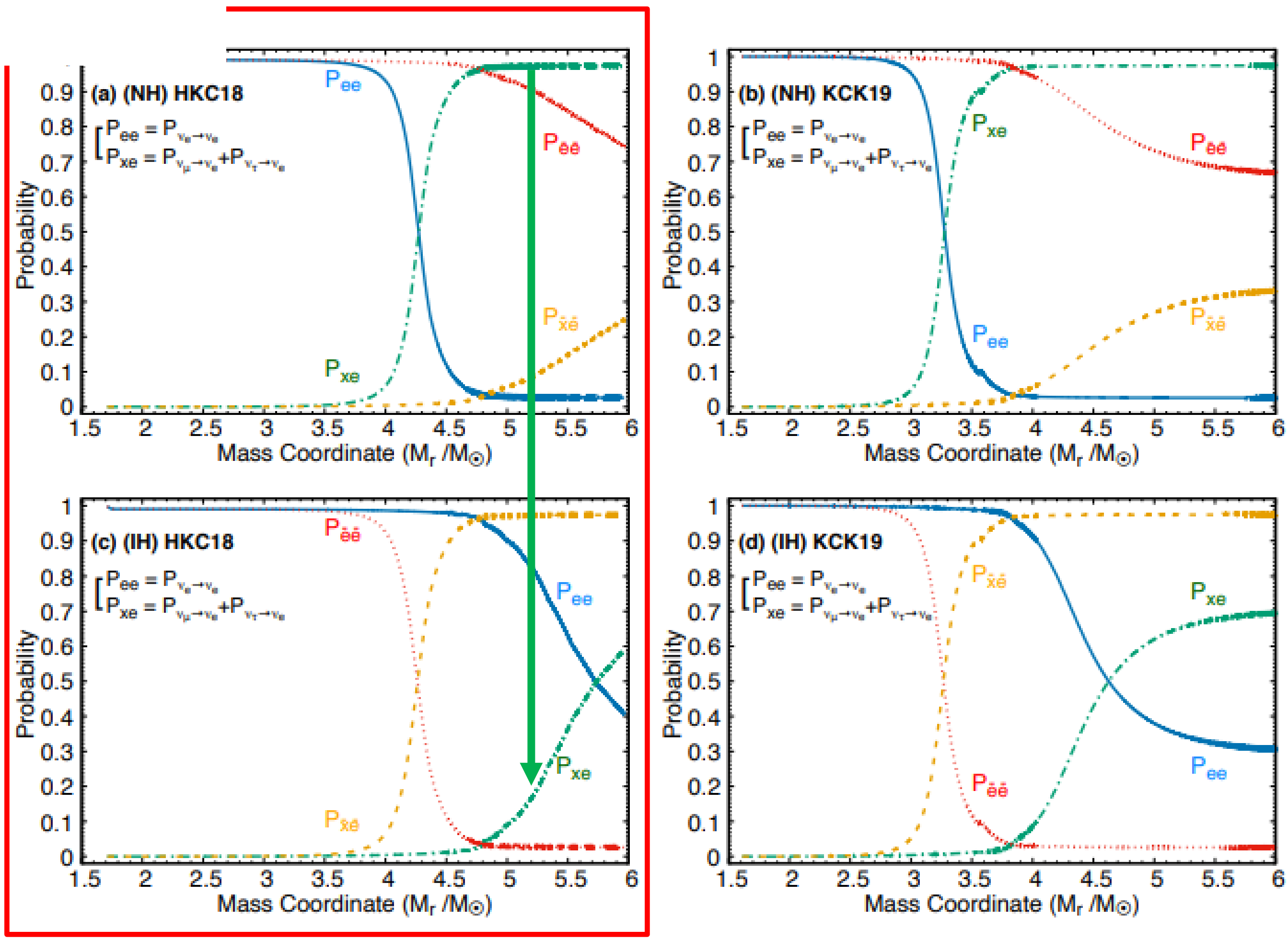


**Figure 4.** The flavor change probability for $\nu_e$ with neutrino energy $E_\nu = 15$ MeV. Left and right panels adopt the hydrodynamics model of *HKC18* (Blinnikov et al. 2000) and *KCK19* (Kusakabe et al. 2019), respectively. Upper and lower panels correspond to the NH and IH, respectively.

# Neutrino Reactions Rates with Nuclei

## Network calculation for nucleosynthesis

$$\frac{dN_j}{dt} = N_i\,\lambda_{i,j} - N_j\,\lambda_{j,h} + \;\ldots \rightarrow \frac{dY_j}{dt} = \boldsymbol{Y_i\,\lambda_{i,j} - Y_j\,\lambda_{j,h}} + \cdots$$

$$Y_j = \frac{N_j}{\rho\,N_A}$$

**JINA REACLIB & Los Alamos (n,g) Data !**

**Kyushu-Tokyo Progenitor Model !**

## Part for neutrino reaction rates

$$\lambda_{\nu_\alpha}(r) = \sigma\,\phi$$
$$= \int_0^\infty \sum_{\alpha=e,\mu,\tau} \frac{d\phi_{\nu_\alpha}}{d\epsilon_\nu}\,Br(\epsilon)\,\sigma_{\nu_\alpha}(\epsilon_\nu)d\epsilon_\nu$$

**Example:**

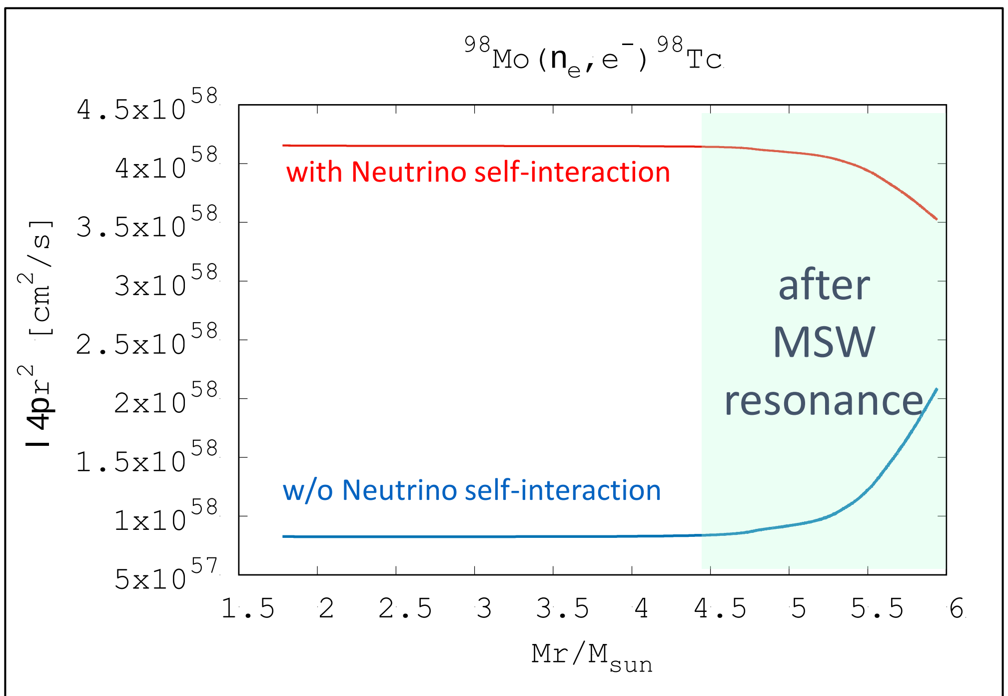


Cross section data using QRPA

TABLE I. Averaged cross sections in units of $10^{-42}$ cm$^2$ for $^{98}$Mo via CC and $^{99}$Ru via NC, and $^{92}$Zr via CC and $^{93}$Nb via NC with particle emission. Neutrino temperatures are taken from [4] and $\langle E_k\rangle$ is calculated from $\langle E_k\rangle/T \sim 3.1514 + 0.1250\alpha$ with $\alpha = 0$ [31,42].

| Reactions | $\langle E_k\rangle$ [MeV] | $T$ [MeV] | $\langle\sigma\rangle$ |
|---|---|---|---|
| $^{98}$Mo$(\nu_e, e^-)^{98}$Tc | 10.08 | 3.2 | 7.77 |
| $^{98}$Mo$(\nu_e, e^- p)^{97}$Mo | 10.08 | 3.2 | 1.90 |
| $^{98}$Mo$(\nu_e, e^- n)^{97}$Tc | 10.08 | 3.2 | 0.09 |
| $^{99}$Ru$(\bar\nu_\mu, \bar\nu'_\mu)^{99}$Ru | 18.90 | 6.0 | 78.5 |
| $^{99}$Ru$(\bar\nu_\mu, \bar\nu'_\mu n)^{98}$Ru | 18.90 | 6.0 | 14.6 |
| $^{99}$Ru$(\bar\nu_\mu, \bar\nu'_\mu p)^{98}$Tc | 18.90 | 6.0 | 1.70 |
| $^{99}$Ru$(\bar\nu_e, \bar\nu'_e)^{99}$Ru | 15.75 | 5.0 | 52.1 |
| $^{99}$Ru$(\bar\nu_e, \bar\nu'_e n)^{98}$Ru | 15.75 | 5.0 | 10.5 |
| $^{99}$Ru$(\bar\nu_e, \bar\nu'_e p)^{98}$Tc | 15.75 | 5.0 | 0.92 |
| $^{92}$Zr$(\nu_e, e^-)^{92}$Nb | 10.08 | 3.2 | 8.92 |

In MSW region, energetic e-neutrino is increased by the x-e neutrino resonance. ( w/o SI)

But it is a bit decreased with the decrease of X-neutrino by the SI )

# Contents

- **Motivation**
- **Neutrino Process in Supernova Explosion**

- **Neutrino Oscillation in vacuum and matter, and neutrino Self-Interaction in the Neutrino Process**
- **Neutrino-induced Reactions by QRPA**
- **Dependence on Neutrino Luminosity**

- **Heavy Elements ($^{92}$Nb,$^{98}$Tc,$^{138}$La,$^{180}$Ta ...)**
- **Light Elements ($^{7}$Li,$^{11}$Be...) & Ratios of $^{7}$Li/$^{11}$B and $^{138}$La/$^{11}$B**

- **Cosmological origin of $^{10}$Be**

- **Sterile Neutrinos & Shock Effects in Neutrino Process**

- **Summary**

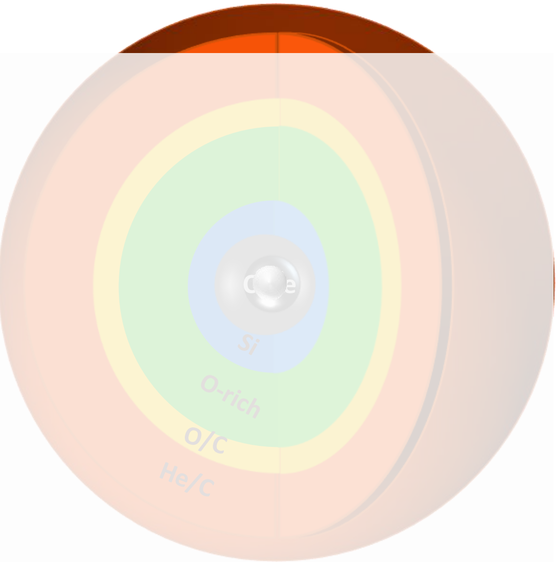

# ν-reaction (2 step) | Data in Low E. region: KARMEN/LSND/CC and NC

Cheoun, Phys. Rev. C 81, 028501 (2010)

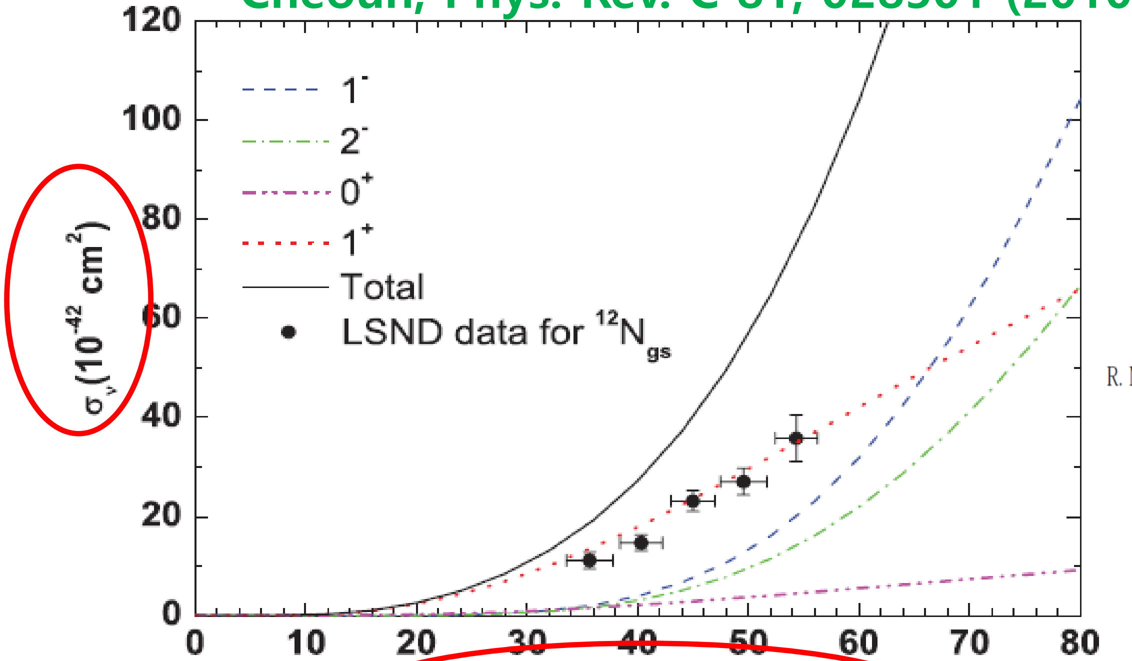


LSND : $\nu_e\,^{12}C \rightarrow e^- + \,^{12}N^*$ $(1^+)$

PHYSICAL REVIEW C, VOLUME 64, 065501

**Measurements of charged current reactions of $\nu_e$ on $^{12}C$**

L. B. Auerbach,[8] R. L. Burman,[5] D. O. Caldwell,[3] E. D. Church,[1] J. B. Donahue,[5] A. Fazely,[7] G. T. Garvey,[5] R. M. Gunasingha,[7] R. Imlay,[6] W. C. Louis,[5] R. Majkic,[8] A. Malik,[6] W. Metcalf,[6] G. B. Mills,[5] V. Sandberg,[5] D. Smith,[4] I. Stancu,[1,*] M. Sung,[6] R. Tayloe,[5,†] G. J. VanDalen,[1] W. Vernon,[2] N. Wadia,[6] D. H. White,[5] and S. Yellin[3]

More data from JSNS$^2$ at JPARC ?

Table 1. Flux-averaged cross sections for neutrinos from $\pi^+$ and $\mu^+$ DAR, measured with KARMEN1 (K1) and KARMEN2 (K2).

| Reaction | $\langle\sigma\rangle$ in $10^{-42}$ cm$^2$ | Comment |
|---|---|---|
| $^{12}C\,(\nu_e, e^-)\,^{12}N_{g.s.}$ | $9.6 \pm 0.3_{(stat)} \pm 0.7_{(syst)}$ | 846 sequences in K1 and K2 |
| $^{12}C\,(\nu, \nu')\,^{12}C^*$ | $10.2 \pm 0.4_{(stat)} \pm 0.8_{(syst)}$ | $\nu = \nu_e, \bar{\nu}_\mu$, K1 and K2 |
| $^{12}C\,(\nu, \nu')\,^{12}C^*$ | $3.2 \pm 0.5_{(stat)} \pm 0.4_{(syst)}$ | $\nu = \nu_\mu$, data from K1 only |
| $^{12}C\,(\nu_e, e^-)\,^{12}N^*$ | $4.8 \pm 0.6_{(stat)}\,^{+0.4}_{-0.5}{}_{(syst)}$ | $\chi^2$-fit on energy spectrum of K2 |
| $^{13}C\,(\nu_e, e^-)\,^{13}N$ | $50 \pm 25_{(stat)}\,^{+4}_{-6}{}_{(syst)}$ | K2 special window evaluation |
| $^{56}Fe\,(\nu_e, e^-)\,X$ | $217 \pm 135_{(stat)}\,^{+27}_{-65}{}_{(syst)}$ | $\chi^2$-fit on energy spectrum of K2 |

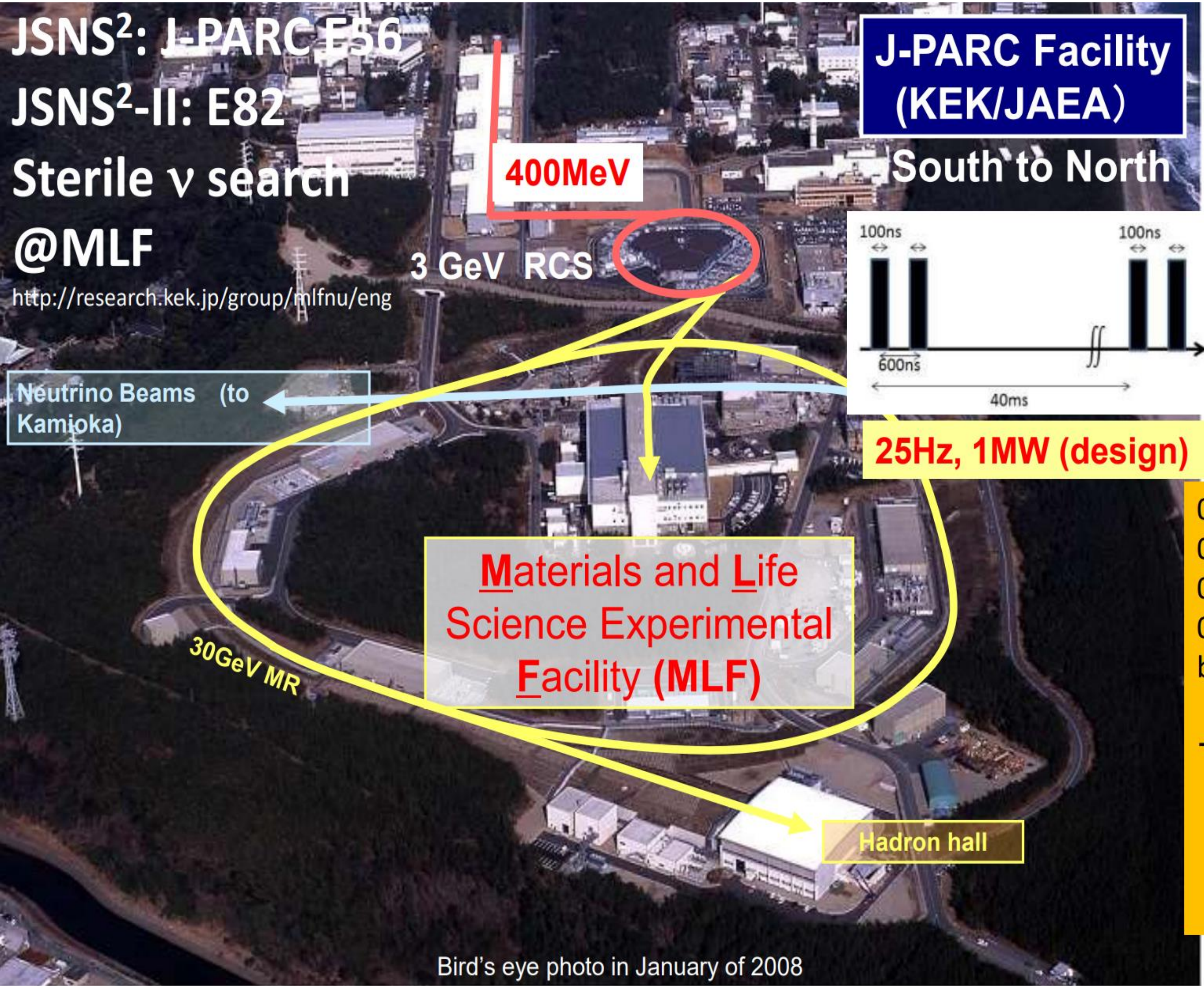


Low duty factor beam (short pulse + low repetition rate) gives excellent S/N ratio.

0.6MW (Jan/12 – Apr/5 2021)
0.7MW (Apr/5 – June/22 2021)
0.7MW (Jan/29 – Apr/5)
0.8MW (Apr/7 – May/31)
beam were utilized for JSNS².

→ Next beam
- starting from 0.8 MW
- electricity costs affect to the available beam time after Nov.

# JSNS$^2$ and JSNS$^2$-II : Sterile Neutrino Search

MLF building (bird's view)

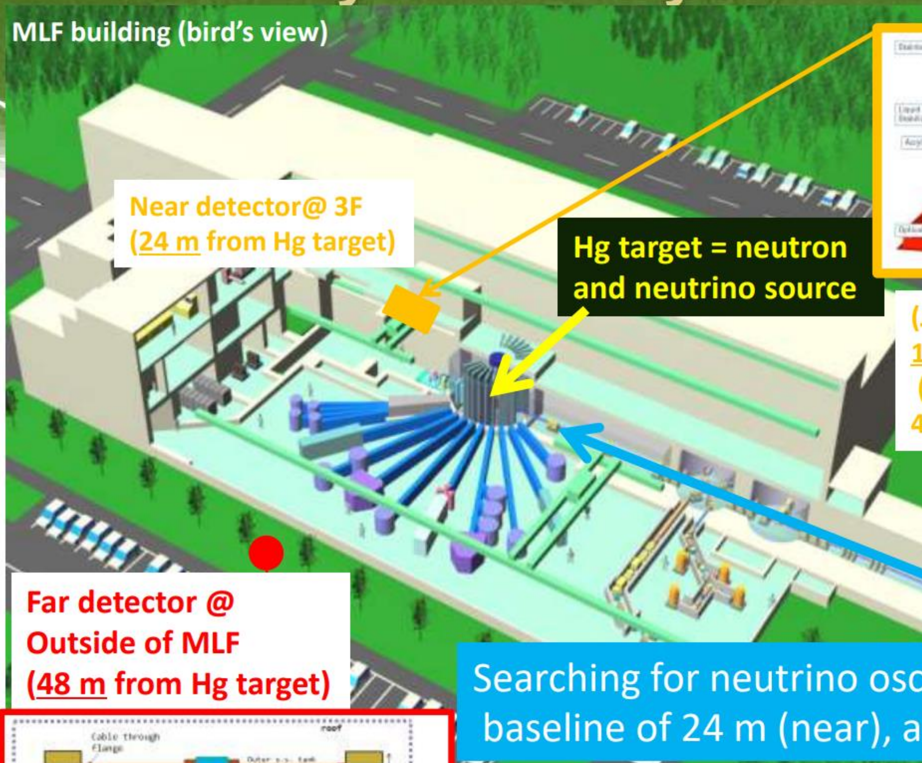

Near detector@ 3F
(24 m from Hg target)

Hg target = neutron and neutrino source


(JSNS2-I, JSNS$^2$-II near detector
17 t GdLS fiducial
(4.6 m diameter x
4.0 m height, 120 10" PMTs)

3GeV short pulsed beam

Far detector @
Outside of MLF
(48 m from Hg target)

Searching for neutrino oscillation : $\overline{\nu_\mu} \rightarrow \overline{\nu_e}$ with baseline of 24 m (near), and 48 m (far detector)

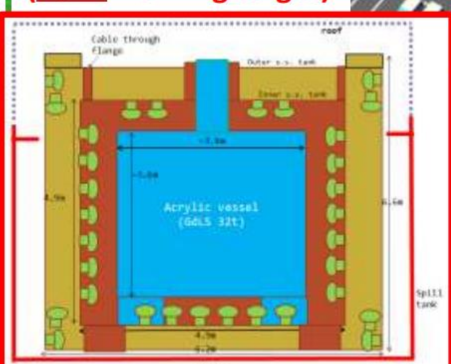


(JSNS$^2$-II:
Far detector)
32 t GdLS
(6.2 m dia x
6.2 m (h)
228 10"
PMTs)

Current JSNS$^2$

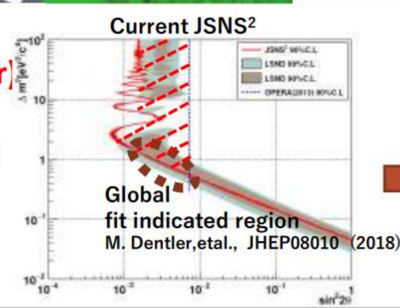


JSNS$^2$-II

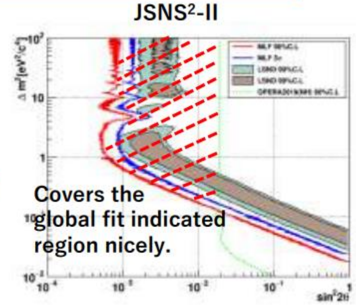


## (JSNS$^2$):1 MW x 3 y(near only)

- Commissioning (2020)
- First long physics run (2021)
  - Smooth data taking (0.5 years)
  - Beam Power: 600-700kW
- Second long physics run (2022)
  - End of Jan to end of May
  - Beam power : 700-800kW

## (JSNS$^2$-II):1 MW x 5 y

- Proposed in 2020 (arXiv:2012.10807)
  - New far detector: fiducial 32 tonnes and 48 m location.
  - Good sensitivity on low $\Delta m^2$ region.
  - Two detectors with two different baselines -> a solid conclusion on LSND anomaly.
  - J-PARC/KEK granted the stage-2 approval.
  - The construction is being progressed rapidly.

### 2.6. Cross sections

Based on the initial and final nuclear states, the cross section for $\nu(\bar{\nu})$–$A$ reactions through the relevant transition operators in equation (27) is given as [30]

$$\left(\frac{d\sigma_\nu}{d\Omega}\right)_{(\nu/\bar{\nu})} = \frac{G_F^2 \epsilon k}{\pi(2J_i+1)}\Bigg[\sum_{J=0}(1+\vec{\nu}\cdot\vec{\beta})|\langle J_f\|\hat{\mathcal{M}}_J\|J_i\rangle|^2 + (1-\hat{\nu}\cdot\vec{\beta}+2(\hat{\nu}\cdot\hat{q})(\hat{q}\cdot\vec{\beta}))|\langle J_f\|\hat{\mathcal{L}}_J\|J_i\rangle|^2 - \hat{q}\cdot(\hat{\nu}+\vec{\beta})2\,\mathrm{Re}\langle J_f\|\hat{\mathcal{L}}_J\|J_i\rangle\langle J_f\|\hat{\mathcal{M}}_J\|J_i\rangle^* + \sum_{J=1}(1-(\hat{\nu}\cdot\hat{q})(\hat{q}\cdot\vec{\beta}))\left(|\langle J_f\|\hat{\mathcal{T}}_J^{el}\|J_i\rangle|^2 + |\langle J_f\|\hat{\mathcal{T}}_J^{mag}\|J_i\rangle|^2\right) \pm \sum_{J=1}\hat{q}\cdot(\hat{\nu}-\vec{\beta})2\,\mathrm{Re}\left[\langle J_f\|\hat{\mathcal{T}}_J^{mag}\|J_i\rangle\langle J_f\|\hat{\mathcal{T}}_J^{el}\|J_i\rangle^*\right]\Bigg], \quad (30)$$

where ($\pm$) means cases of $\nu$ ($\bar{\nu}$). $\vec{\nu}$ and $\vec{k}$ are three-momenta of incident and final leptons, and $\vec{q} = \vec{k} - \vec{\nu}$, $\vec{\beta} = \vec{k}/\epsilon$ with the final lepton's energy $\epsilon$. Of course, the extremely relativistic limit (ERL) may yield more simple formula, but we use the general expression in order to apply for $\nu_\mu$–$A$ reactions. For the CC reaction we multiplied the Cabbibo angle $\cos^2\theta_c$ and include the Coulomb distortion of outgoing leptons due to residual nuclei [3, 10].

**Phys. Rev. C99, (2019), 064304;**
**Phys. Rev. C97, (2018), 064322;**
**Phys. Rev. C97, (2018), 024320;**
**EPJA 53, (2017), 26 ….**
**JPG, 46 (2019), 105109**

**For neutrino-nuclei reactions,**

1. We include the transition from 0(+/-) up to 4(+/-) !!!
2. To describe the excitations of compound nuclei, we exploit the (D)QRPA.
3. In the QRPA, the Brueckner G matrix based on the CD Bonn potential and 'all kinds of pairing interactions' in the BCS are included.
4. These (D)QRPA have been successfully tested to reproduce **the GT strength distr.**.
5. For the excitation spectrum of the compound nuclei, we exploit a statistical model by S. Chiba in TIT.

$$\hat{\mathcal{M}}_{JM;TM_T}(q\mathbf{x}) = \left\{ F_1^{(T)} M_J^{M_J}(q\mathbf{x}) - i\frac{q}{M}\left[ F_A^{(T)}\Omega_J^{M_J}(q\mathbf{x}) + \frac{F_A - \omega F_P^{(T)}}{2}\Sigma''^{M_J}_J(q\mathbf{x})\right]\right\} I_T^{M_T},$$

$$\hat{\mathcal{L}}_{JM;TM_T}(q\mathbf{x}) = \left[\frac{-\omega}{q} F_1^{(T)} M_J^{M_J}(q\mathbf{x}) + i\left(F_A^{(T)} - \frac{q^2}{2M_N}F_P^{(T)}\right)\Sigma''^{M_J}_J(q\mathbf{x})\right] I_T^{M_T},$$

$$\hat{\mathcal{T}}^{\mathrm{el}}_{JM;TM_T}(q\mathbf{x}) = \left\{\frac{q}{M}\left[F_1^{(T)}\Delta'^{M_J}_J(q\mathbf{x}) + \frac{1}{2}\mu^{(T)}\Sigma_J^{M_J}(q\mathbf{x})\right] + iF_A^{(T)}\Sigma'^{M_J}_J(q\mathbf{x})\right\} I_T^{M_T},$$

$$\hat{\mathcal{T}}^{\mathrm{mag}}_{JM;TM_T}(q\mathbf{x}) = -i\frac{q}{M}\left\{\left[F_1^{(T)}\Delta_J^{M_J}(q\mathbf{x}) - \frac{1}{2}\mu^{(T)}\Sigma'^{M_J}_J(q\mathbf{x})\right] + F_A^{(T)}\Sigma_J^{M_J}(q\mathbf{x})\right\} I_T^{M_T},$$

Matrix elements of any transition operator can be factored in QRPA as follows

$$\langle \mathrm{QRPA}\|\hat{\mathcal{O}}_\lambda\|\omega; JM\rangle = [\lambda]^{-1}\sum_{ab}\langle a\|\hat{\mathcal{O}}_\lambda\|b\rangle\langle \mathrm{QRPA}\|[c_a^+\tilde{c}_b]_\lambda\|\omega; JM\rangle, \tag{6}$$

where $\langle a\|\hat{\mathcal{O}}_\lambda\|b\rangle$ can be evaluated for a given single-particle basis independently of nuclear models. For the second factor, ground states assumed as the BCS state and excited states generated from the ground state by the phonon operator of Eq. (3) are exploited with the quasiboson approximation.

# Coupled (nn + pp + np) DQRPA by np pairing

$$
\begin{pmatrix}
A^{1111}_{\alpha\beta\gamma\delta}(K) & A^{1122}_{\alpha\beta\gamma\delta}(K) & A^{1112}_{\alpha\beta\gamma\delta}(K) & B^{1111}_{\alpha\beta\gamma\delta}(K) & B^{1122}_{\alpha\beta\gamma\delta}(K) & B^{1112}_{\alpha\beta\gamma\delta}(K) \\
A^{2211}_{\alpha\beta\gamma\delta}(K) & A^{2222}_{\alpha\beta\gamma\delta}(K) & A^{2212}_{\alpha\beta\gamma\delta}(K) & B^{2211}_{\alpha\beta\gamma\delta}(K) & B^{2222}_{\alpha\beta\gamma\delta}(K) & B^{2212}_{\alpha\beta\gamma\delta}(K) \\
A^{1211}_{\alpha\beta\gamma\delta}(K) & A^{1222}_{\alpha\beta\gamma\delta}(K) & A^{1212}_{\alpha\beta\gamma\delta}(K) & B^{1211}_{\alpha\beta\gamma\delta}(K) & B^{1222}_{\alpha\beta\gamma\delta}(K) & B^{1212}_{\alpha\beta\gamma\delta}(K) \\
-B^{1111}_{\alpha\beta\gamma\delta}(K) & -B^{1122}_{\alpha\beta\gamma\delta}(K) & -B^{1112}_{\alpha\beta\gamma\delta}(K) & -A^{1111}_{\alpha\beta\gamma\delta}(K) & -A^{1122}_{\alpha\beta\gamma\delta}(K) & -A^{1112}_{\alpha\beta\gamma\delta}(K) \\
-B^{2211}_{\alpha\beta\gamma\delta}(K) & -B^{2222}_{\alpha\beta\gamma\delta}(K) & -B^{2212}_{\alpha\beta\gamma\delta}(K) & -A^{2211}_{\alpha\beta\gamma\delta}(K) & -A^{2222}_{\alpha\beta\gamma\delta}(K) & -A^{2212}_{\alpha\beta\gamma\delta}(K) \\
-B^{1211}_{\alpha\beta\gamma\delta}(K) & -B^{1222}_{\alpha\beta\gamma\delta}(K) & -B^{1212}_{\alpha\beta\gamma\delta}(K) & -A^{1211}_{\alpha\beta\gamma\delta}(K) & -A^{1222}_{\alpha\beta\gamma\delta}(K) & -A^{1212}_{\alpha\beta\gamma\delta}(K)
\end{pmatrix}
\times
\begin{bmatrix}
\tilde{X}^m_{(\gamma 1 \delta 1)K} \\
\tilde{X}^m_{(\gamma 2 \delta 2)K} \\
\tilde{X}^m_{(\gamma 1 \delta 2)K} \\
\tilde{Y}^m_{(\gamma 1 \delta 1)K} \\
\tilde{Y}^m_{(\gamma 2 \delta 2)K} \\
\tilde{Y}^m_{(\gamma 1 \delta 2)K}
\end{bmatrix}
= \hbar \Omega^m_K
\begin{pmatrix}
\tilde{X}^m_{(\alpha 1 \beta 1)K} \\
\tilde{X}^m_{(\alpha 2 \beta 2)K} \\
\tilde{X}^m_{(\alpha 1 \beta 2)K} \\
\tilde{Y}^m_{(\alpha 1 \beta 1)K} \\
\tilde{Y}^m_{(\alpha 2 \beta 2)K} \\
\tilde{Y}^m_{(\alpha 1 \beta 2)K}
\end{pmatrix},
$$

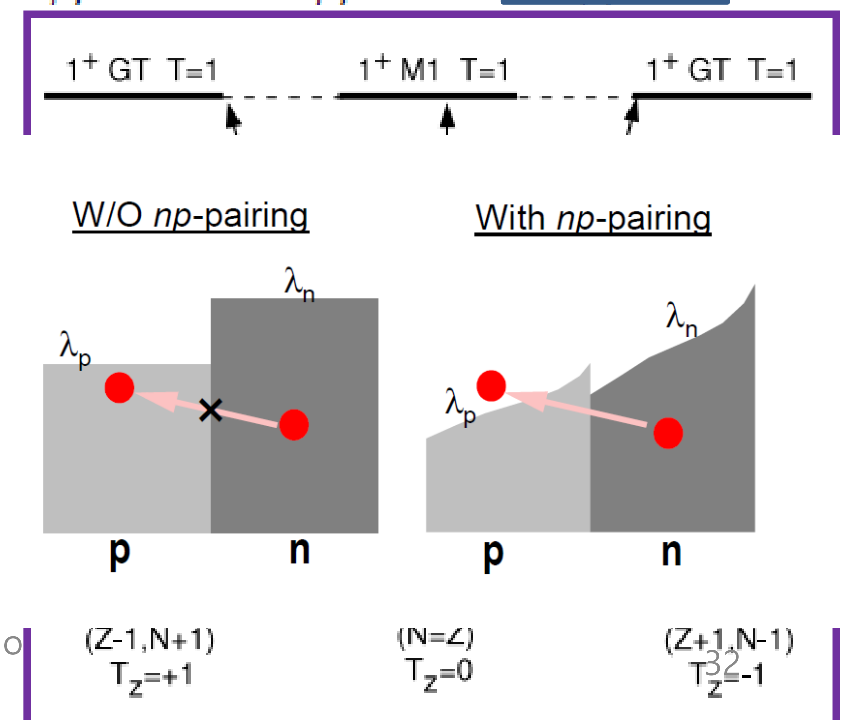

# Contents

The first University in Korea
Soongsil University



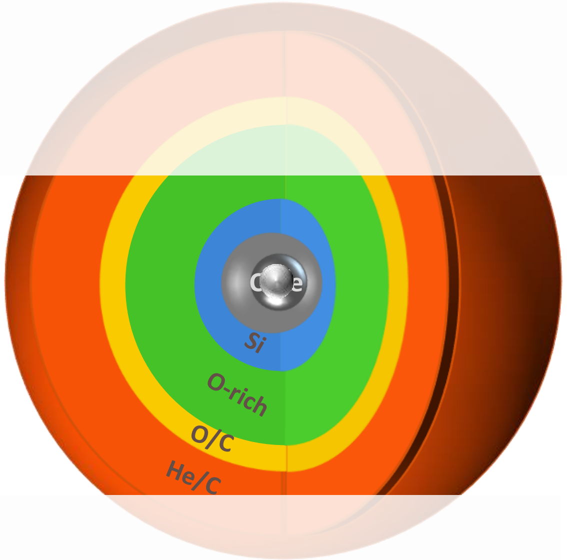

JINA REALIB

Modified (n,g) Reactions

QRPA & Branching Ratios

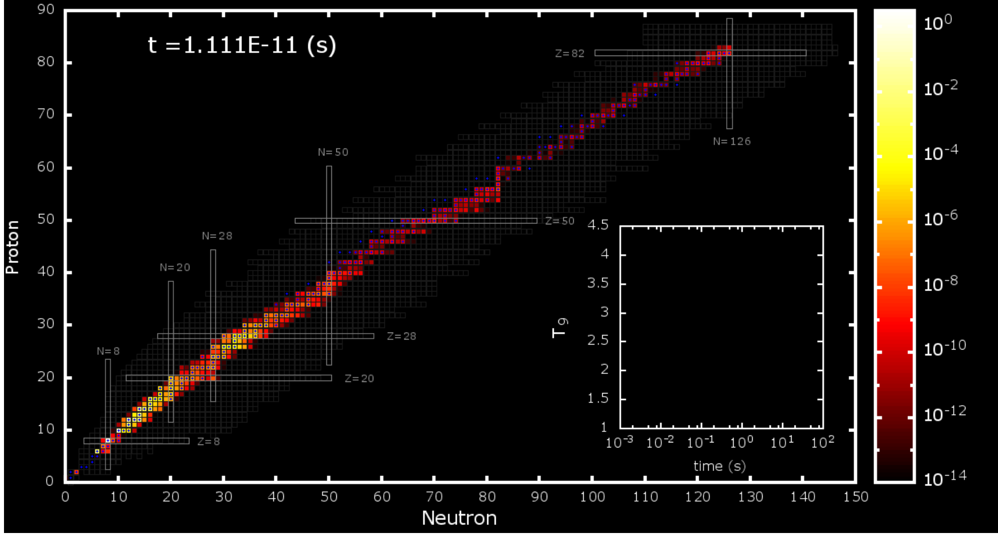


# Numerical results for elements abundances

1987 SN model

Pre-supernova Model

Hydrodynamics Model

Modified Neutrino Flux by Self-interaction

Neutrino Luminosity

Flavor change probability by shock wave and others

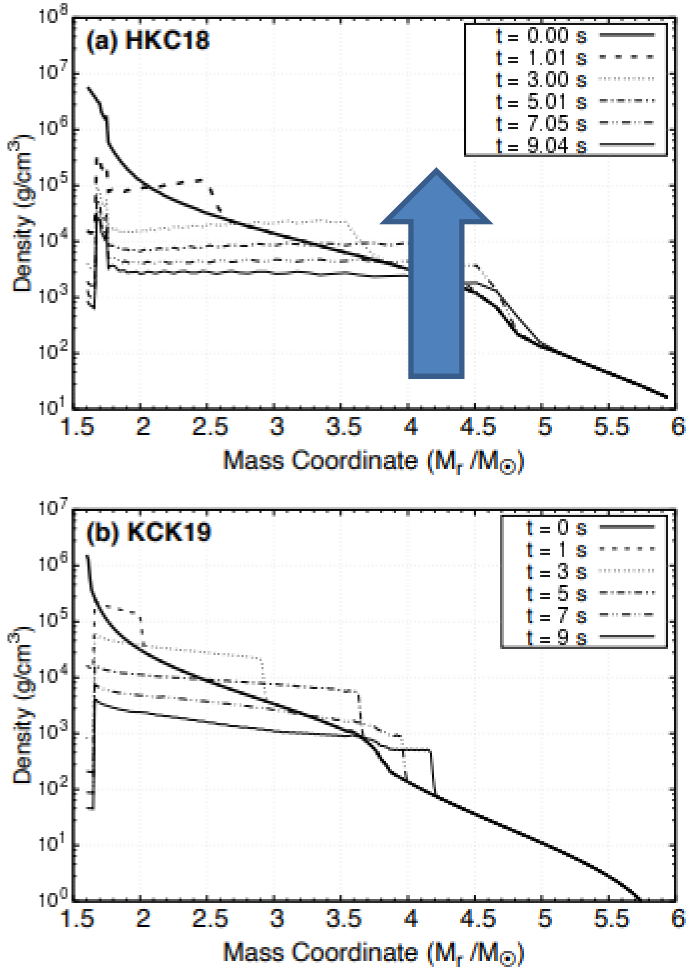


**Figure 1.** The time-evolving density profiles in the Lagrange mass coordinate. The upper and lower panels show the hydrodynamics models used in *HKC18* (Blinnikov et al. 2000) and *KCK19* (Kusakabe et al. 2019), respectively. The time range is taken from about 0 to 7 seconds.

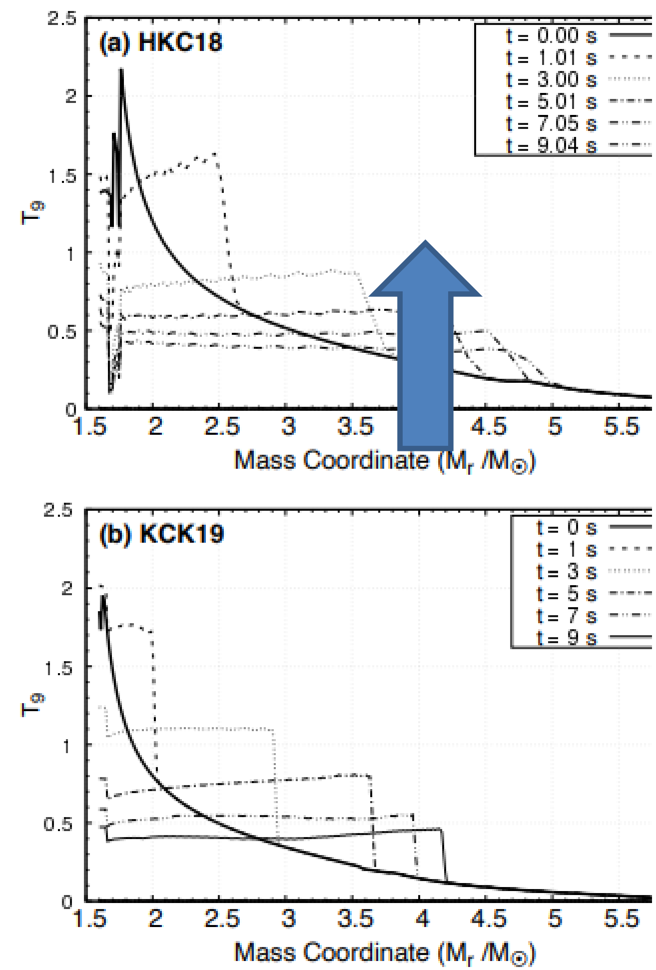


**Figure 2.** The time-evolving temperature profiles as a tion of the Lagrange mass coordinate. The upper and panels adopt the same models in Figure 1, respectively temperature unit is taken as $T_9 = T/(10^9\ \mathrm{K})$.

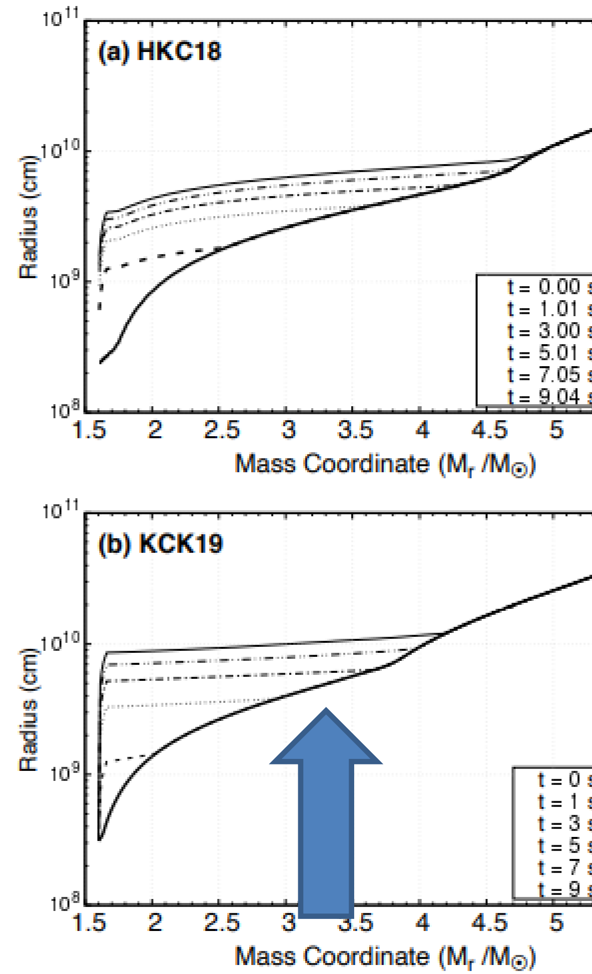


**Figure 3.** The time-evolving radius profiles as a the Lagrange mass coordinate. The upper and lo adopt the same models in Figure 1, respectively.

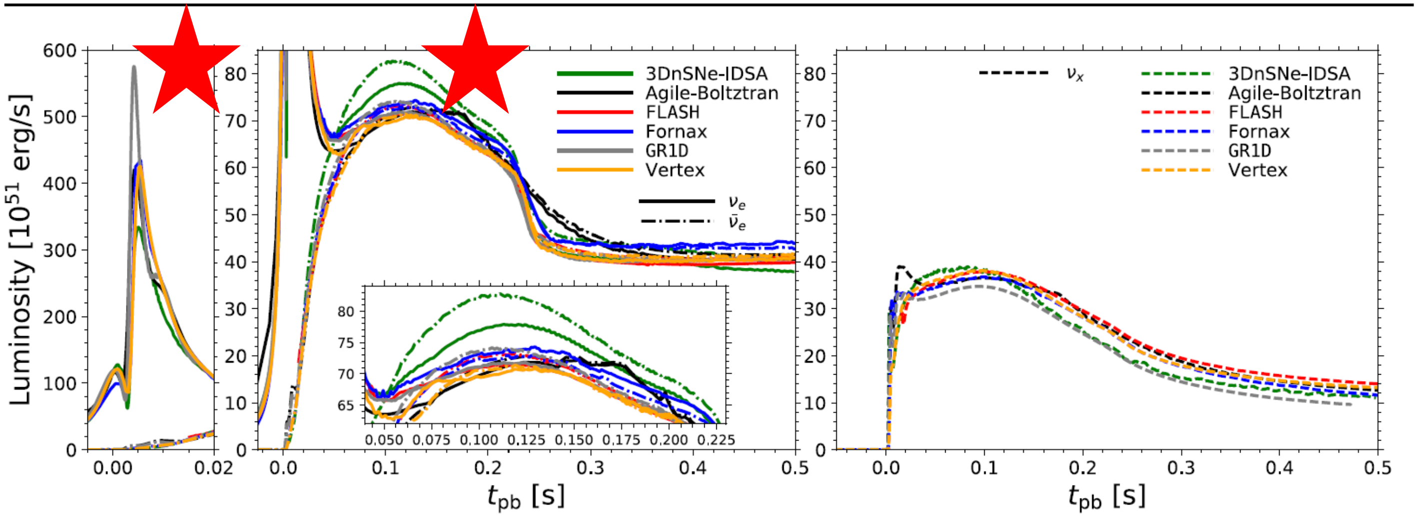


**Figure 3.** Neutrino luminosities as a function of postbounce time. In the left panels we show electron-type neutrino luminosities (solid lines show electron neutrinos while dashed–dotted lines show electron antineutrinos) and in the right panel we show the characteristic heavy-lepton neutrino luminosity (dashed line). For clarity, we show an inset to highlight the early accretion epoch for the electron-type neutrinos and a panel to show the neutronization burst. Some curves have been smoothed with neighboring zones to remove noise and improve clarity.

*3.1. 3DnSNe-IDSA*

*Contributors*: *Tomoya Takiwaki, Kei Kotake*

*3.2. AGILE-BOLTZTRAN*

*Contributors*: *Tobias Fischer, Eric Lentz, Matthias Liebendörfer, Bronson Messer, Anthony Mezzacappa*The radiation-hydrodynamics module AGILE is based on the spherically-sym-

*3.3. FLASH-M1*

*Contributors*: *Evan O'Connor, Sean Couch*

*3.4. FORNAX*

*Contributors*: *Adam Burrows, David Vartanyan*

*3.5. GR1D*

*Contributors*: *Evan O'Connor*

*3.6. PROMETHEUS-VERTEX*

*Contributors*: *Robert Bollig, Hans-Thomas Janka*

J. Phys. G: Nucl. Part. Phys. **45** (2018) 104001 E O'Connor *et al*

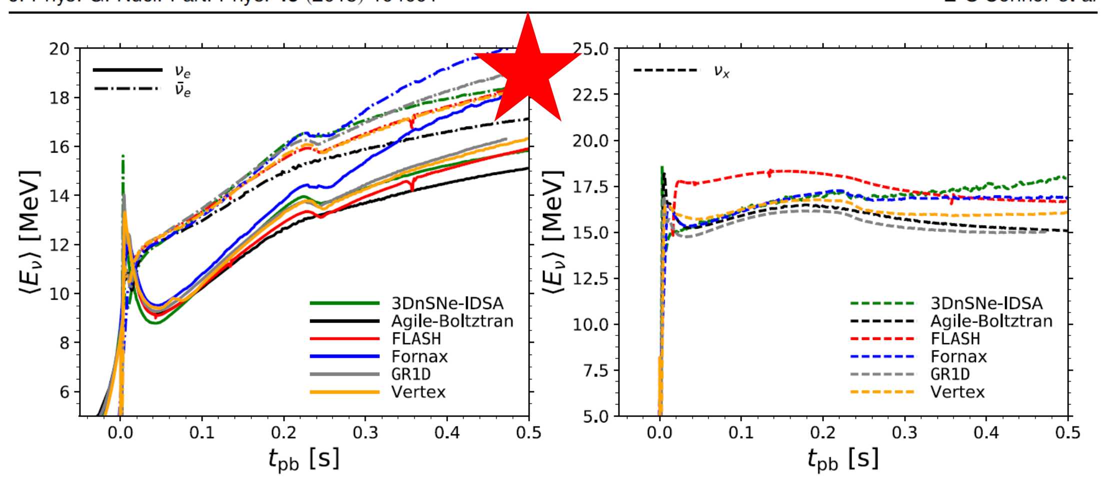


**Figure 4.** Neutrino average energy as a function of postbounce time. In the left panel we show electron-type neutrino average energies (solid lines show electron neutrinos while dashed–dotted lines show electron antineutrinos) and in the right panel we show

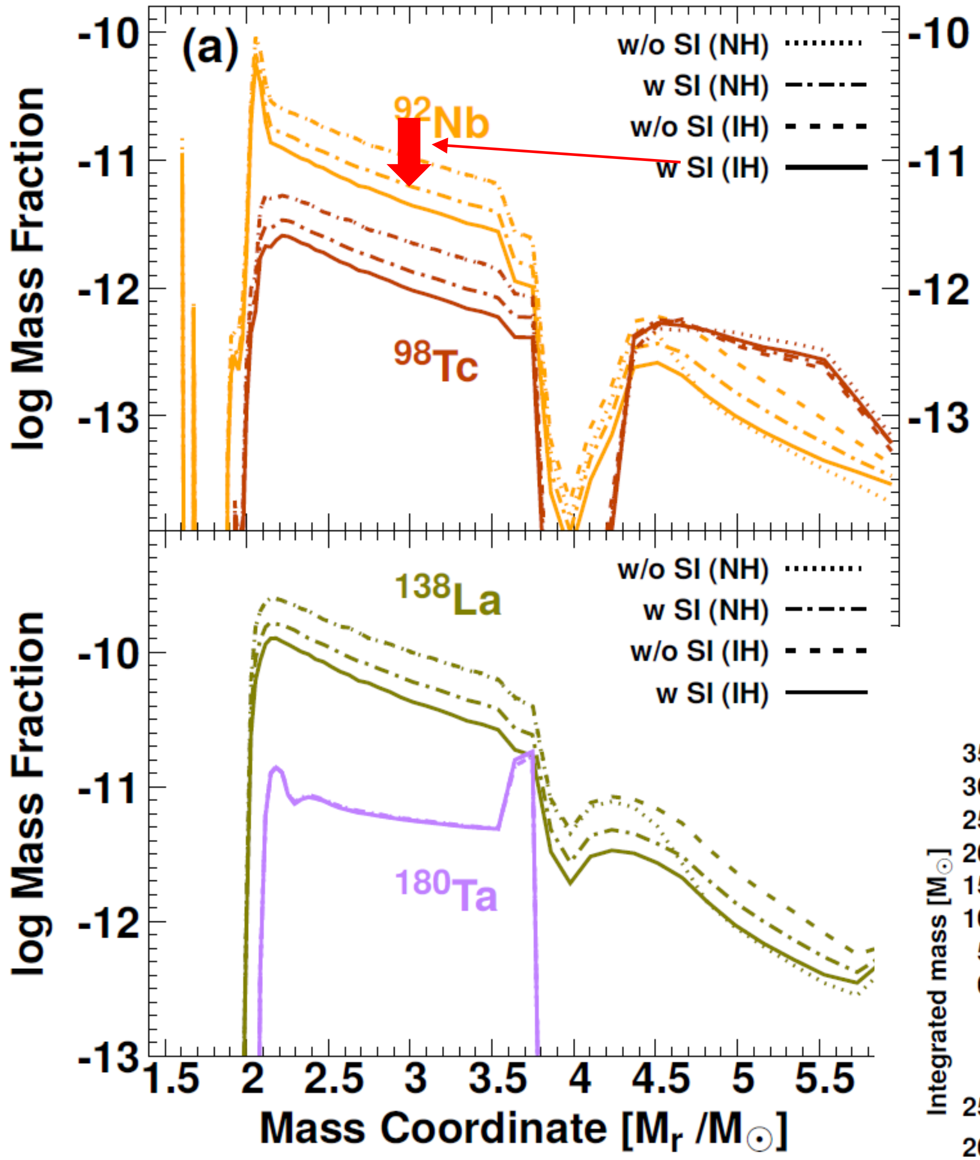
(a)
w/o SI (NH)
w SI (NH)
w/o SI (IH)
w SI (IH)
92Nb
98Tc
138La
180Ta
log Mass Fraction
Mass Coordinate [Mr /M⊙]
-10
-11
-12
-13
1.5
2
2.5
3
3.5
4
4.5
5
5.5

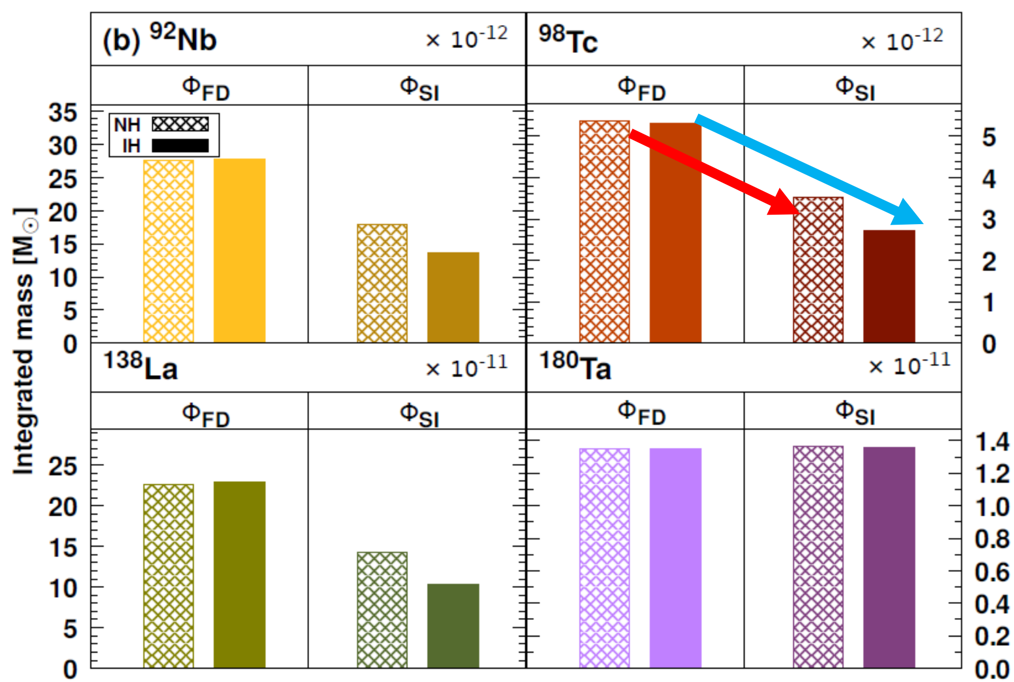
(b) 92Nb × 10-12
98Tc × 10-12
138La × 10-11
180Ta × 10-11
ΦFD
ΦSI
NH
IH
Integrated mass [M⊙]

# Neutrino process Results for Light Elements II

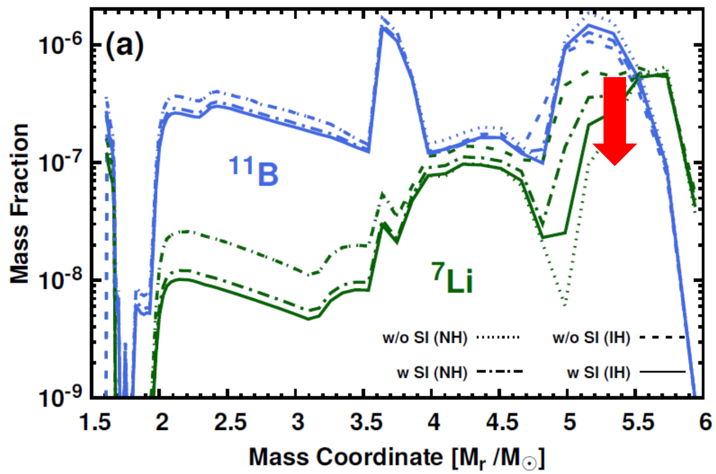


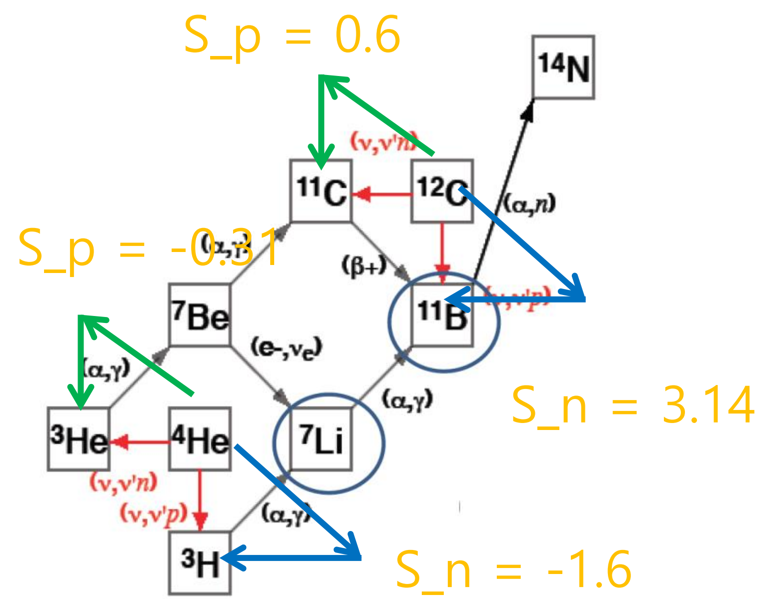


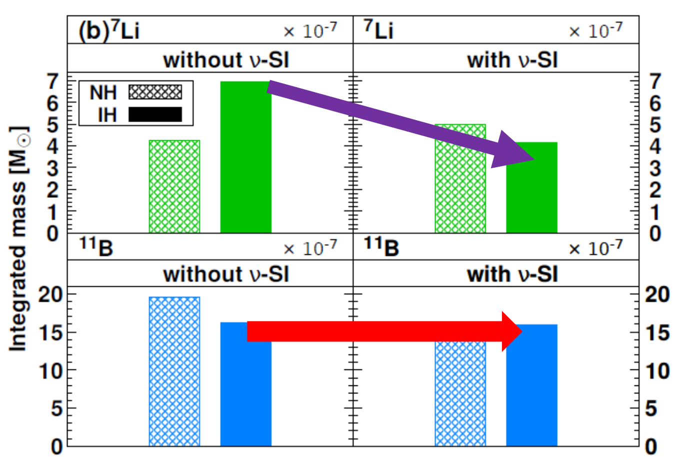


For 7Li, the main reactions are
both e- and anti-e- CC reactions
which are larger than NC.
And e-CC through 3He and 7Be
from 4He is larger than anti-e due to MSW.
=> Sensitive on the nu-SI.

But for 11B both electro-
and antielectron-neutrinos CC and NC work.
=> Insensitive to the nu-SI.

Hydrodynamics : HKC18 and KCK19
Luminosity : EQ and NEQ
Neutrino Self Interaction : FD and SI
Mass Hierarchy : NH and IH

**Table 4:** Integrated masses of the nuclei after 50 s in the mass range, $M_r = 1.6$–$6$ ($M_\odot$). We used two hydrodynamics models (HKC18 and KCK19), two luminosity models (EQ and NEQ) and two cases without the $\nu$−SI (FD) and with the $\nu$−SI (SI) for the NH and IH case, by which the results for twelve different cases are tabulated. The last two results are quoted from our previous results. See texts for the details.

| | Mass Hierarchy | $^7$Li | $^7$Be | $^{11}$B | $^{11}$C | $^{92}$Nb | $^{98}$Tc | $^{138}$La | $^{180}$Ta | Yield ratio | PF ratio |
|---|---|---|---|---|---|---|---|---|---|---|---|
| | | ($10^{-7}$ $M_\odot$) | | | | ($10^{-12}$ $M_\odot$) | | ($10^{-11}$ $M_\odot$) | | N($^7$Li)/N($^{11}$B) | $^{138}$La/$^{11}$B |
| FD EQ (HKC18) | NH | 1.256 | 4.953 | 5.576 | 2.048 | 4.903 | 1.048 | 3.395 | 0.845 | 1.280 | 0.1288 |
| | IH | 1.496 | 1.461 | 7.141 | 1.218 | 4.760 | 1.112 | 3.267 | 0.843 | 0.556 | 0.1130 |
| FD EQ (KCK19) | NH | 0.861 | 2.428 | 2.480 | 2.139 | 4.551 | 1.180 | 3.760 | 1.016 | 1.119 | 0.2354 |
| | IH | 1.017 | 0.936 | 3.099 | 0.883 | 4.226 | 1.218 | 3.436 | 1.012 | 0.771 | 0.2495 |
| FD EQ Shock (KCK19) | NH | 0.861 | 1.904 | 2.546 | 1.701 | 4.973 | 1.271 | 4.164 | 1.017 | 1.023 | 0.2835 |
| | IH | 0.949 | 1.027 | 2.922 | 0.937 | 4.271 | 1.215 | 3.485 | 1.012 | 0.805 | 0.2611 |
| SI EQ[a] (KCK19) | NH | 0.861 | 2.428 | 2.480 | 2.139 | 4.551 | 1.180 | 3.760 | 1.016 | 1.119 | 0.2354 |
| | IH | 0.920 | 2.057 | 2.852 | 3.874 | 15.07 | 3.259 | 13.58 | 1.052 | 0.695 | 0.5838 |
| SI NEQ (KCK19) | NH | 1.132 | 1.601 | 4.276 | 4.920 | 16.44 | 3.559 | 15.19 | 1.295 | 0.467 | 0.4776 |
| | IH | 1.261 | 1.206 | 4.623 | 4.283 | 12.29 | 2.854 | 11.31 | 1.281 | 0.435 | 0.3672 |
| FD NEQ (KCK19) | NH | 1.483 | 0.841 | 5.407 | 5.258 | 25.44 | 5.367 | 23.14 | 1.323 | 0.342 | 0.6274 |
| | IH | 0.959 | 2.303 | 3.946 | 6.566 | 26.15 | 5.302 | 23.94 | 1.331 | 0.488 | 0.6585 |
| SI NEQ Ko et al. (2020) (HKC18) | NH | 1.643 | 3.347 | 9.332 | 6.138 | 17.92 | 3.511 | 14.29 | 1.363 | 0.507 | 0.2671 |
| | IH | 1.792 | 2.372 | 10.33 | 5.524 | 13.59 | 2.720 | 10.41 | 1.358 | 0.413 | 0.1899 |
| FD NEQ Ko et al. (2020) (HKC18) | NH | 2.400 | 1.860 | 12.46 | 7.080 | 27.56 | 5.361 | 22.62 | 1.349 | 0.343 | 0.335 |
| | IH | 1.640 | 5.270 | 8.382 | 7.804 | 27.83 | 5.318 | 22.94 | 1.353 | 0.671 | 0.410 |

[a]Same as FD EQ (KCK19) NH result

THE ASTROPHYSICAL JOURNAL LETTERS, 891:L24 (6pp), 2020 March 1 https://doi.org/10.3847/2041-8213/ab775b


CrossMark

# Neutrino Process in Core-collapse Supernovae with Neutrino Self-interaction and MSW Effects

Heamin Ko[1], Myung-Ki Cheoun[1], Eunja Ha[1], Motohiko Kusakabe[2], Takehito Hayakawa[3], Hirokazu Sasaki[4], Toshitaka Kajino[2,4], Masa-aki Hashimoto[5], Masaomi Ono[6], Mark D. Usang[7], Satoshi Chiba[7], Ko Nakamura[8], Alexey Tolstov[9], Ken'ichi Nomoto[9], Toshihiko Kawano[10], and Grant J. Mathews[11]

# Mass Fraction ratio of 7Li/11B and PF ration of 138La/11B

- The yield ratio of [7Li/11B]

$^7Li/^{11}B = -0.31 \pm 0.42$ **<0.53 (2 sigma)**

| Spectra | FD | +SI | FD | +SI |
|---|---|---|---|---|
| Mass Hierarchy | IH | IH | NH | NH |
| Yield Ratio | 0.671(0.488) | 0.413(0.435) | 0.343(0.342) | 0.507(0.467) |

- The production factor ratio of [138La/11B] **< 0.41**

$PF[A] = X_A / X_{A\odot}$ with $X_A$ the mass fraction of A

| Spectra | FD | +SI | FD | +SI |
|---|---|---|---|---|
| Mass Hierarchy | IH | IH | NH | NH |
| PF ratio | 0.410(0.6585) | 0.1899(0.3672) | 0.335(0.6274) | 0.2671(0.4776) |

# NH is favored !!!

However, is this the last story ?
but
the least ??? Other effects ?

# Contents

- Motivation
- Neutrino Process in Supernova Explosion
- Neutrino Oscillation in vacuum and matter, and neutrino Self-Interaction in the Neutrino Process
- Neutrino-induced Reactions by QRPA
- Dependence on Neutrino Luminosity
- Heavy Elements ($^{92}Nb$, $^{98}Tc$, $^{138}La$, $^{180}Ta$ …)
- Light Elements ($^{7}Li$, $^{11}Be$…) & Ratio of $^{11}B/^{138}La$
- **Cosmological origin of $^{10}Be$**
- Sterile Neutrinos & Shock Effects in Neutrino Process
- Summary

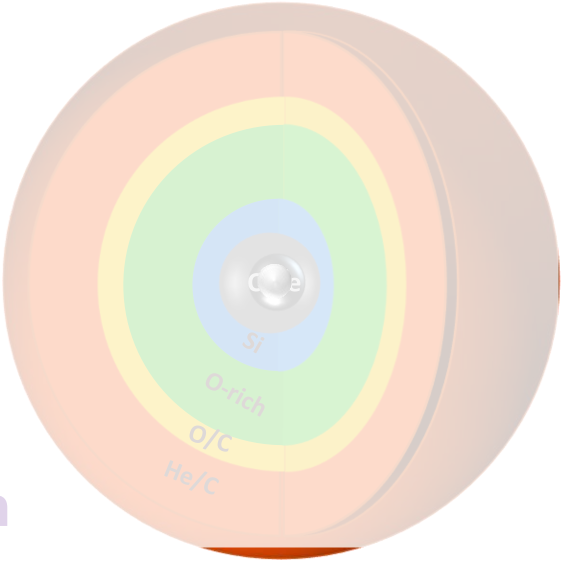

# Introduction - meteorite data

- 논문에 있는 운식 데이터를 비교

*Nature Communications, (2016), 7*

nature COMMUNICATIONS

ARTICLE

Received 14 Jan 2016 | Accepted 20 Oct 2016 | Published 22 Nov 2016 DOI: 10.1038/ncomms13639 OPEN

## Evidence from stable isotopes and $^{10}Be$ for solar system formation triggered by a low-mass supernova

Projjwal Banerjee[1], Yong-Zhong Qian[1], Alexander Heger[2,3] & W.C. Haxton[4]

About 4.6 billion years ago, some event disturbed a cloud of gas and dust, triggering the gravitational collapse that led to the formation of the solar system. A core-collapse supernova, whose shock wave is capable of compressing such a cloud, is an obvious candidate for the initiating event. This hypothesis can be tested because supernovae also produce telltale patterns of short-lived radionuclides, which would be preserved today as isotopic anomalies. Previous studies of the forensic evidence have been inconclusive, finding a pattern of isotopes differing from that produced in conventional supernova models. Here we argue that these difficulties either do not arise or are mitigated if the initiating supernova was a special type, low in mass and explosion energy. Key to our conclusion is the demonstration that short-lived $^{10}Be$ can be readily synthesized in such supernovae by neutrino interactions, while anomalies in stable isotopes are suppressed.

10Be can produced from the SN !

# Introduction - meteorite data

- 논문에 있는 운석 데이터를 비교

*Nature Communications, (2016), 7*

Meteorite

**Table 1 | Yields of short-lived radionuclides from an 11.8-solar-mass core-collapse supernova.**

| R/I | $\tau_R$ (Myr) | $Y_R$ ($M_\odot$) | $X_I^\odot$ | $(N_R/N_I)_{ESS}$ | | | |
|---|---|---|---|---|---|---|---|
| | | | | Data | Case 1 | Case 2 | Case 3 |
| $^{10}Be/^{9}Be$ | 2.00 | 3.26( − 10) | 1.40( − 10) | (7.5 ± 2.5)( − 4) | 6.35( − 4) | 6.35( − 4) | 5.20( − 4) |
| $^{26}Al/^{27}Al$ | 1.03 | 2.91( − 6) | 5.65( − 5) | (5.23 ± 0.13)( − 5) | 1.02( − 5) | 9.90( − 6) | 5.77( − 6) |
| $^{36}Cl/^{35}Cl$ | 0.434 | 1.44( − 7) | 3.50( − 6) | ~(3-20)( − 6) | 2.00( − 6) | 1.45( − 6) | 6.15( − 7) |
| $^{41}Ca/^{40}Ca$ | 0.147 | 3.66( − 7) | 5.88( − 5) | (4.1 ± 2.0)( − 9) | 3.40( − 9) | 2.74( − 9) | 2.26( − 9) |
| $^{53}Mn/^{55}Mn$ | 5.40 | 1.22( − 5) | 1.29( − 5) | (6.28 ± 0.66)( − 6) | 4.04( − 4) | 6.39( − 6) | 6.16( − 6) |
| $^{60}Fe/^{56}Fe$ | 3.78 | 3.08( − 6) | 1.12( − 3) | ~1( − 8);(5-10)( − 7) | 9.80( − 7) | 9.80( − 7) | 1.10( − 7) |
| $^{107}Pd/^{108}Pd$ | 9.38 | 1.37( − 10) | 9.92( − 10) | (5.9 ± 2.2)( − 5) | 6.27( − 5) | 6.27( − 5) | 5.72( − 5) |
| $^{135}Cs/^{133}Cs$ | 3.32 | 2.56( − 10) | 1.24( − 9) | ~5( − 4) | 7.51( − 5) | 7.51( − 5) | 3.18( − 5) |
| $^{182}Hf/^{180}Hf$ | 12.84 | 4.04( − 11) | 2.52( − 10) | (9.72 ± 0.44)( − 5) | 7.36( − 5) | 7.36( − 5) | 6.34( − 6) |
| | | 8.84( − 12) | | | 1.60( − 5) | 1.60( − 5) | 2.37( − 6) |
| $^{205}Pb/^{204}Pb$ | 24.96 | 9.20( − 11) | 3.47( − 10) | ~1( − 4);1( − 3) | 1.27( − 4) | 1.27( − 4) | 7.78( − 5) |

Comparisons are made to the corresponding isotopic ratios deduced from meteoritic data. Case 1 estimates are calculated from equation (1) using the approximate best-fit $f$ and $\Delta$ of Fig. 2, assuming no fallback. The higher and lower yields for $^{182}Hf$ are obtained from the laboratory and estimated stellar decay rates[47] of $^{181}Hf$, respectively. Case 2 (3) is a fallback scenario in which only 1.5% of the innermost $1.02 \times 10^{-2}$ solar mass (0.116 solar mass) of shocked material is ejected. With guidance from refs 22,31, well-determined data are quoted with $2\sigma$ errors, while data with large uncertainties are preceded by '~'. Note that $x(-y)$ denotes $x \times 10^{-y}$. Data references are: $^{10}Be$ (refs 14,16,18,19), $^{26}Al$ (refs 2,32), $^{36}Cl$ (refs 33-35), $^{41}Ca$ (refs 36,37), $^{53}Mn$ (ref. 38), $^{60}Fe$ (refs 39,40), $^{107}Pd$ (ref. 41), $^{135}Cs$ (ref. 42), $^{182}Hf$ (ref. 43) and $^{205}Pb$ (refs 44,45).

particles (SEPs[10,11]) associated with activities of the proto-Sun. It was noted in Yoshida *et al.*[12] that $^{10}Be$ can be produced by neutrino interactions in CCSNe, but the result was presented for a single model and no connection to meteoritic data was made. Further, that work adopted an old rate for the destruction reaction $^{10}Be(\alpha,n)^{13}C$ that is orders of magnitude larger than currently recommended[13], and therefore, greatly underestimated the $^{10}Be$ yield.

$^{10}Be$ has been observed in the form of a $^{10}B$ excess in a range of meteoritic samples. Significant variations across the samples

Group Meeting July 8th 2022

13. Cyburt, R. H. *et al.* The JINA REACLIB database: its recent updates and impact on type-I X-ray bursts. *Astrophys. J. Suppl. Ser.* **189**, 240–252 (2010).

They reported that the data of the ratio 10Be/9Be was obtained from the meteorite analysis.
Note that 10Be is unstable and 9Be is stable.
But previous calculation predicted that 10Be cannot be produced by the neutrino-process because the destruction channel 10Be(a,n)13C was overestimated i.e. 10Be was destructed fully.

# Direct measurement of Li and Be isotope ratios in Cosmic-rays onboard a satellite

ApJ 862:141 (2018).

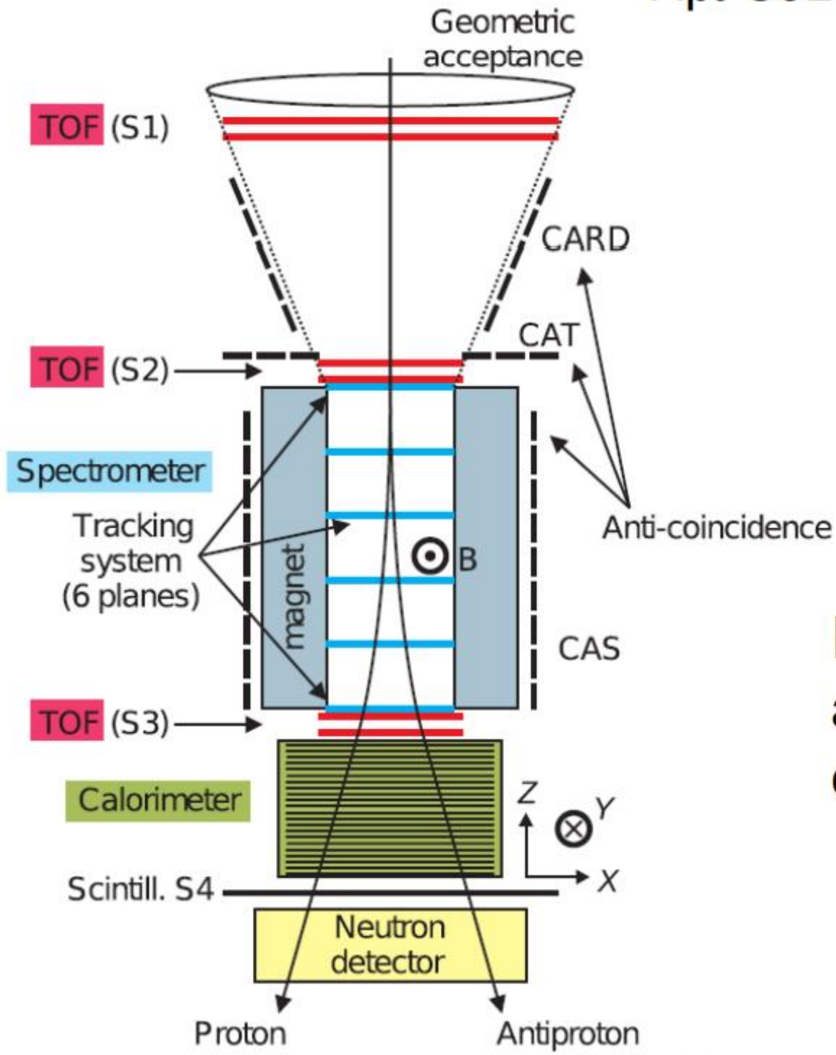


**Figure 1.** Scheme of the detectors composing the PAMELA satellite experiment.

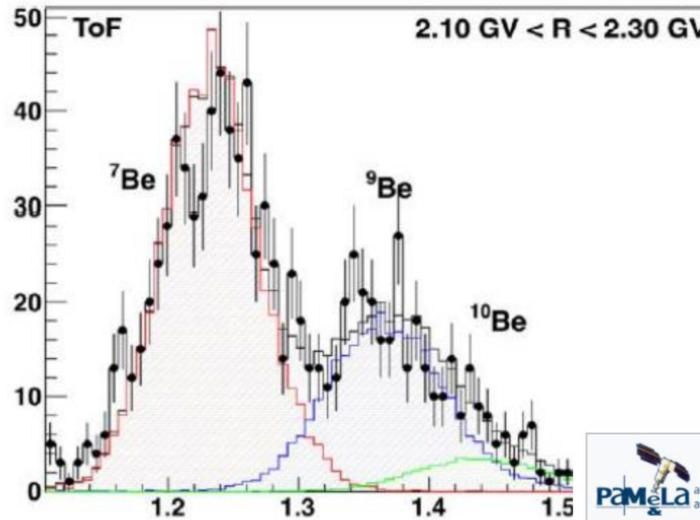


It is assumed that Li an Be
are predominantly produc
cosmic-rays in these proje

**PAMELA**

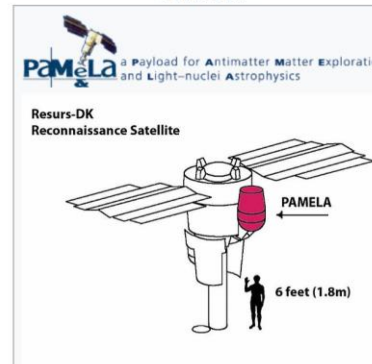


| | |
|---|---|
| Organization | PAMELA group |
| Mission Type | Cosmic Ray |
| Host Satellite | Resurs DK1 |
| Launch | 15 June 2006 |
| Launch vehicle | Soyuz-FG |
| Launch site | Baikonur Cosmodrome |
| Mission duration | 3 years (planned), over 9 years achieved |
| Mission end | 7 February 2016 |
| Mass | 470 kg |
| Max length | 1300 mm |
| Power consumption | 335 Watts |

# Introduction

- Short-lived Radioactive Nuclei

*Progress in Particle and Nuclear Physics, (2018), 1-47, 102*

**Table 3**
List of stellar nucleosynthesis sites and the nucleosynthetic processes occurring within them that are responsible for the production of the SLRs and stable reference isotopes listed in Column 3. Column 4 indicates if the site of production is important in terms of GCE (**M**=Major) or not (*m*=minor); **M**/*m* indicates that it is still debated whether the site is major or minor. Indicative references are listed in Column 5.

| Stellar site | Process | Products | Relevance | Ref. |
|---|---|---|---|---|
| Low-mass AGBs | *s* process | $^{107}$Pd, $^{108}$Pd | **M** | [93,94] |
| | | $^{135}$Cs, $^{133}$Cs | **M** | |
| | | $^{182}$Hf, $^{180}$Hf | **M** | |
| | | $^{205}$Pb, $^{204}$Pb | **M** | |
| Massive and Super-AGBs | p captures | $^{26}$Al | *m* | [80,94–96] |
| | n captures | $^{41}$Ca, $^{36}$Cl, $^{60}$Fe | *m* | |
| | *s* process | $^{107}$Pd, $^{135}$Cs, $^{182}$Hf | *m* | |
| WR stars | p captures | $^{26}$Al | **M** | [97,98] |
| | n captures | $^{41}$Ca, $^{36}$Cl | *m* | |
| | n captures | $^{97}$Tc, $^{107}$Pd, $^{135}$Cs, $^{205}$Pb | *m* | |
| CCSNe | p captures+explosive | $^{26}$Al, $^{27}$Al | **M** | [99] |
| | n captures | $^{60}$Fe | **M** | [99] |
| | n captures | $^{36}$Cl, $^{41}$Ca | **M** | [94,100] |
| | C/Ne/O burning | $^{35}$Cl, $^{40}$Ca | **M** | [101] |
| | NSE | $^{53}$Mn, $^{55}$Mn, $^{56}$Fe | **M**/*m*[a] | [101] |
| | n captures | $^{107}$Pd, $^{126}$Sn, $^{135}$Cs | *m* | [102] |
| | | $^{129}$I, $^{182}$Hf, $^{205}$Pb | *m* | |
| | $\alpha$-rich freezeout | $^{92}$Nb, $^{92}$Mo, $^{97}$Tc, $^{98}$Tc | **M**/*m* | [103] |
| | $\gamma$ process | $^{144}$Sm, $^{146}$Sm | **M**/*m* | [103,104] |
| | $\nu$ process | $^{10}$Be, $^{92}$Nb | *m* | [105,106] |
| SNIa | NSE | $^{53}$Mn, $^{55}$Mn, $^{56}$Fe | **M** | [107] |
| | $\gamma$ process | $^{92}$Nb, $^{93}$Nb, $^{146}$Sm, $^{144}$Sm | **M**/*m* | [108] |
| | | $^{97}$Tc, $^{98}$Tc, $^{98}$Ru | **M**/*m* | |
| NSMs/special CCSNe | *r* process | $^{107}$Pd, $^{108}$Pd, $^{126}$Sn, $^{124}$Sn | **M** | [109][b] |
| | | $^{135}$Cs, $^{133}$Cs, $^{129}$I, $^{127}$I | **M** | |
| | | $^{182}$Hf, $^{180}$Hf | **M** | |
| | | $^{247}$Cm, $^{235}$U, $^{244}$Pu, $^{238}$U | **M** | [110,111] |
| novae | p captures | $^{26}$Al | *m* | [112] |
| CRs | non-thermal | $^{7}$Be, $^{10}$Be, $^{9}$Be | **M** | [32] |
| | | $^{26}$Al, $^{41}$Ca, $^{36}$Cl, $^{53}$Mn | *m* | [113] |

[a] The current understanding is that roughly 1/3 of the abundances of the Fe-peak elements in the Galaxy are produced by CCSNe, with the rest coming from SNIa.
[b] Abundances to be derived using the *s*-process predictions provided in the reference via the *r*-residual method, where the *r*-process abundance is given by the Solar System abundance minus the *s*-process abundance.

~~Group Meeting July 8th 2022~~

*[105] Nature Communications, (2016), 7*

But, even if we use the correct rate for the (a,n) reaction,
the production rate is smaller than the production by the cosmic ray, which is a kind of the spallation by cosmic rays.

That is the reason why the main mechanism is the spallation by the CR. Is it true?

# Production of 10Be in the neutrino-process

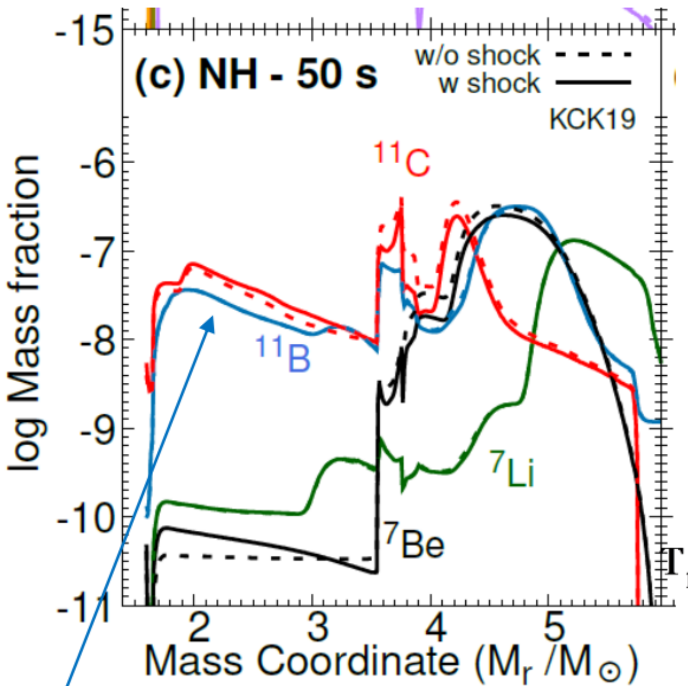


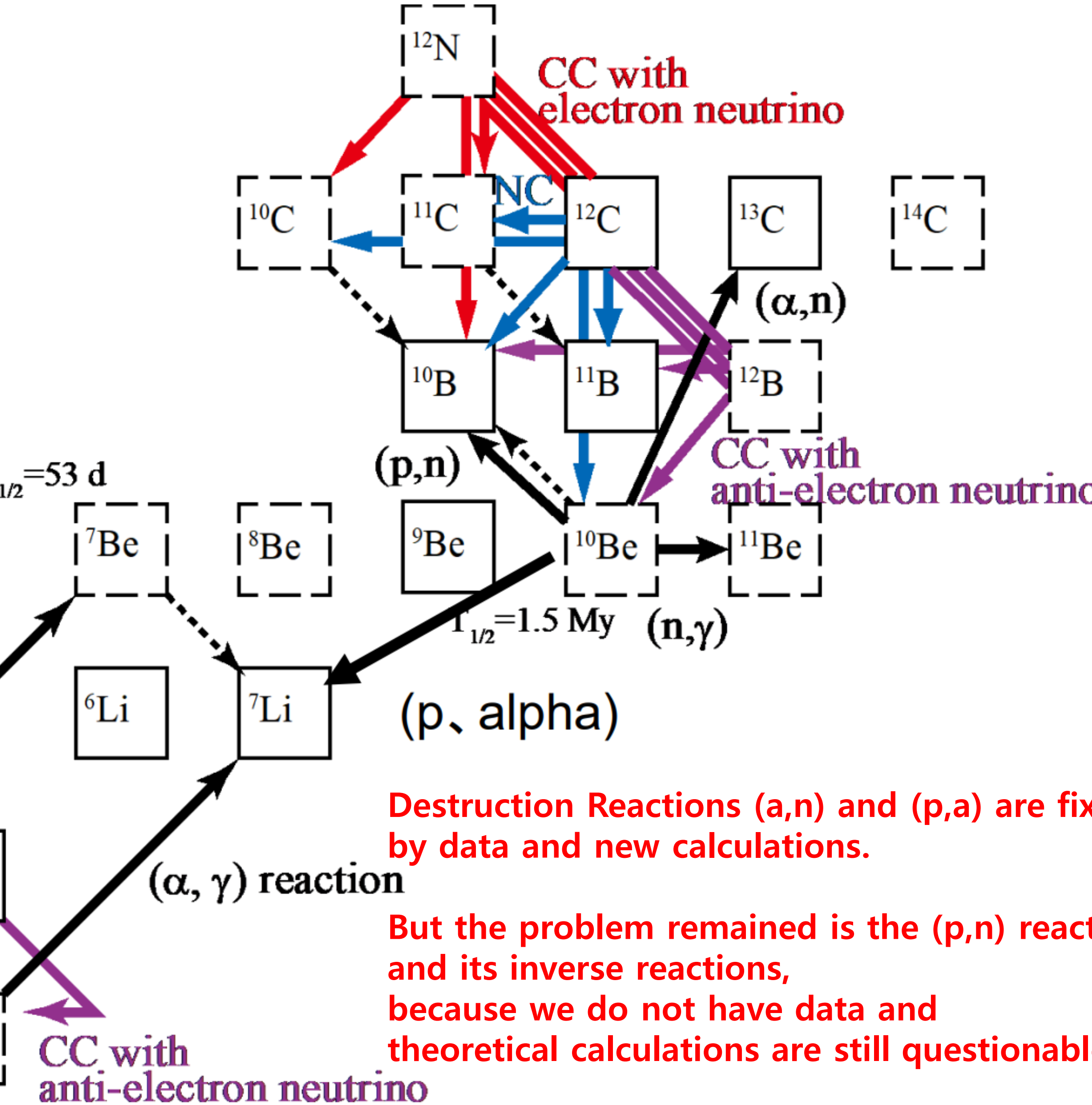


The yield of 10Be is expected to be similar to 11B

**Destruction Reactions (a,n) and (p,a) are fixed by data and new calculations.**

**But the problem remained is the (p,n) reaction and its inverse reactions, because we do not have data and theoretical calculations are still questionable.**

# Mass Coordinate vs Mass Fraction

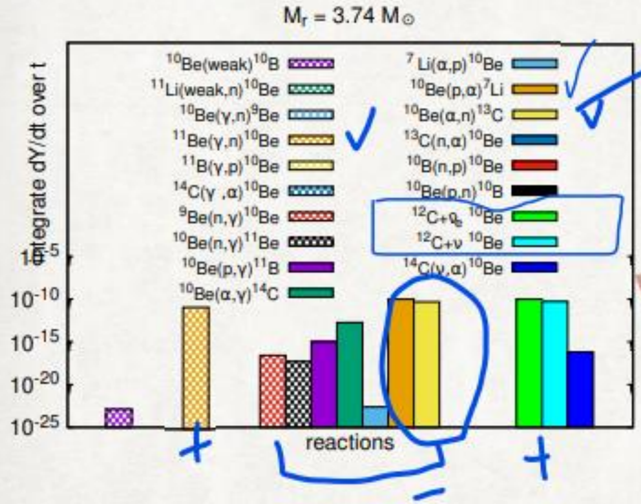


Main production

$$^{12}\mathrm{C} + \bar{\nu}_e \rightarrow {}^{10}\mathrm{Be}$$

Main destruction

$$^{10}\mathrm{Be}(p,\alpha)^{7}\mathrm{Li}$$

Not me

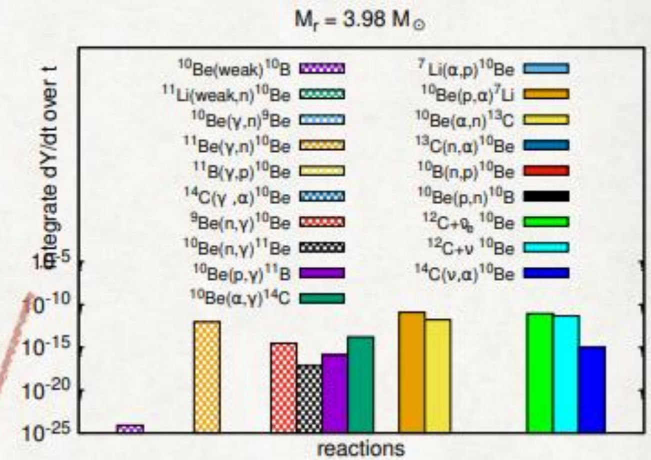


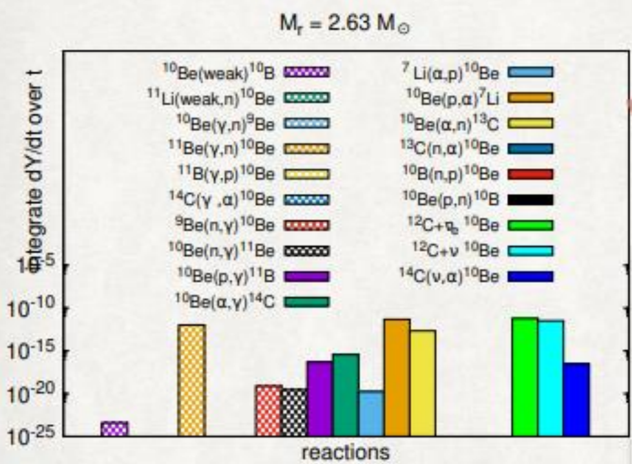


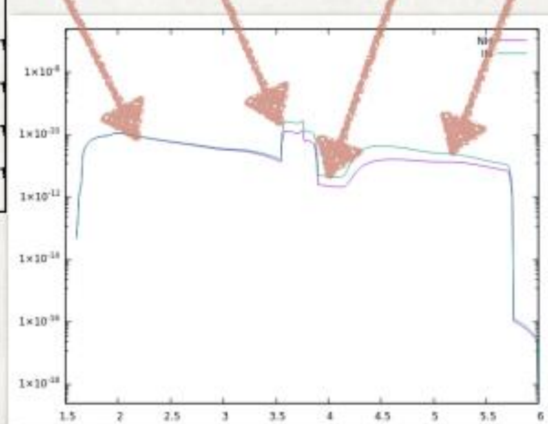

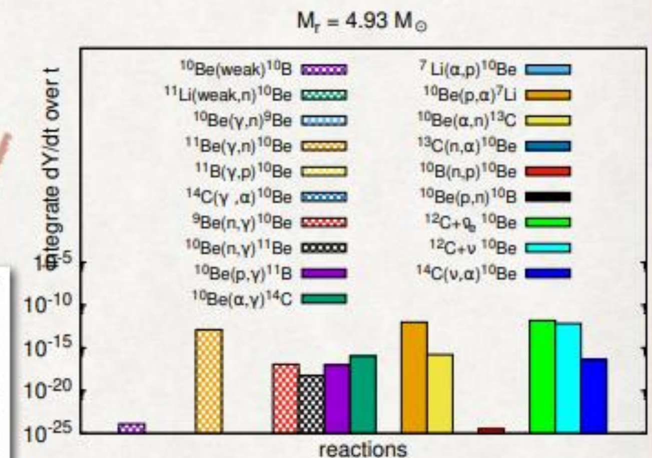


$^{10}$Be(p,n)$^{10}$B contr. is small, but very impor.

Histograms for NH case

이전 계산은 $^{10}$Be이 O(-22) 정도로 작았음

~~Group Meeting July 8th 2022~~

**(n,p) and (p,n) reactions**
**by Talys which was used in the process**

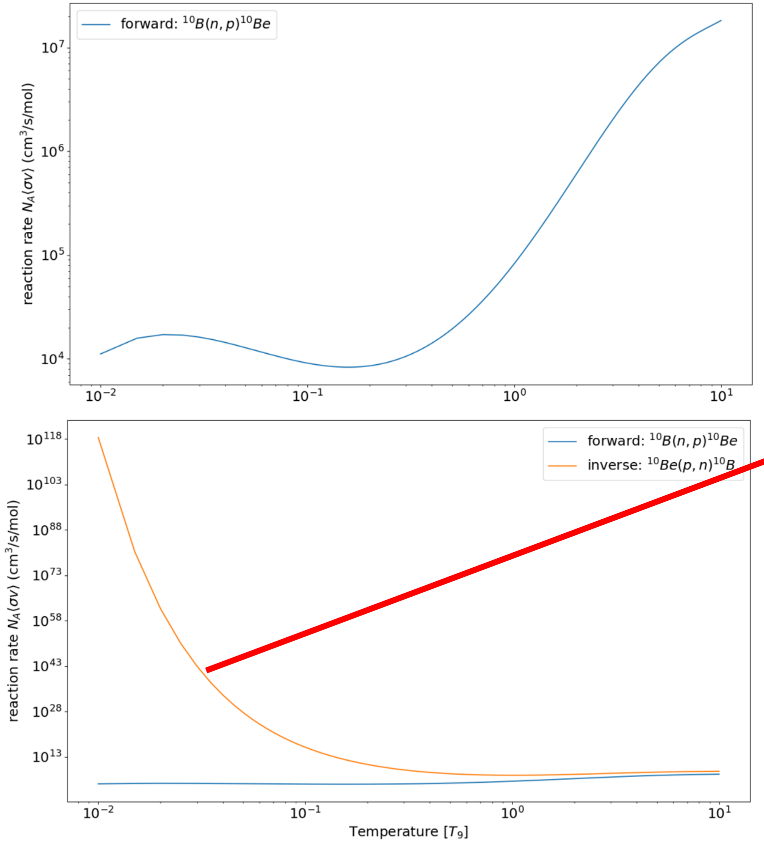


(0.01 T9 < T <10 T9)

0.00086 MeV (= 0.086 keV) < E < 0.86 MeV)

1MeV=1.16*10^10 Kelvin

Destruction reaction 10Be(p,n)10B is too large.
It is calculated by Talys !

That is the reason 10Be was too small O(-22)
in the previous calculation which used the Talys results!!

# Forward Reaction and inverse reaction

## Cross section

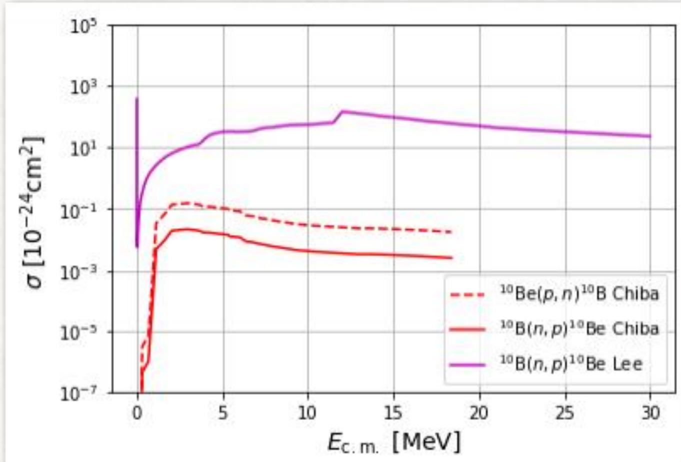


## Thermonuclear reaction rate

*The index "kusa" denotes TALYS-1.8 code (2015) in Kusakabe et al, APJ, (2019), 164, 872 (2)*

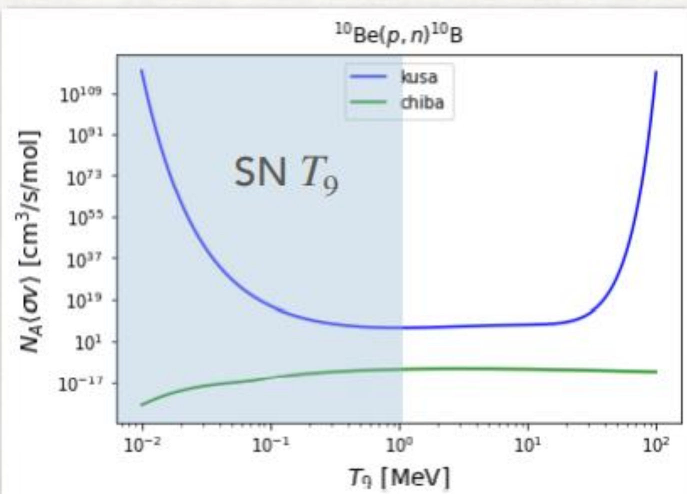


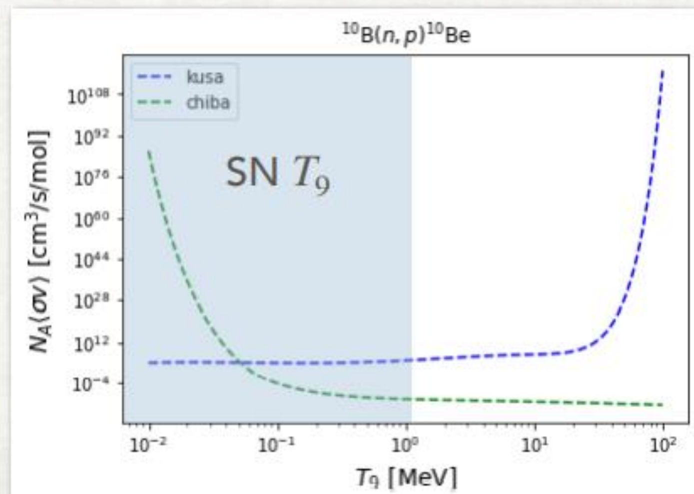


~~Group Meeting July 8th 2022~~

If we use the new data for the (n,p) and (p,n) reactions deduced from JENDL data,
The destruction becomes small, and the construction is larger than those by the Talys. **Be10 abundance is up !!**

## Previous calculation

t~50s

| | | $^{10}$Be and $^{53}$Mn | | | | $^{9}$Be and $^{55}$Mn |
|---|---|---|---|---|---|---|
| R/I | Mass hierarchy | Life time (Myr) | Mass yield **ONeMg** | Mass yield **He (+C/O)** | Mass yield | Solar abundance (Lodders et al. 2009) |
| $^{10}$Be/$^{9}$Be | NH | 2.00 | 6.672E-26 | 2.444E-24 | 2.51072E-24 | 1.5088E-10 |
| | IH | 2.00 | 4.802E-21 | 2.170E-23 | 4.8237E-21 | 1.5088E-10 |
| $^{53}$Mn/$^{55}$Mn | NH | 5.40 | 5.383E-08 | 2.638E-09 | 5.6468E-08 | 1.3891E-05 |
| | IH | 5.40 | 5.303E-08 | 1.324E-09 | 5.4354E-08 | 1.3891E-05 |

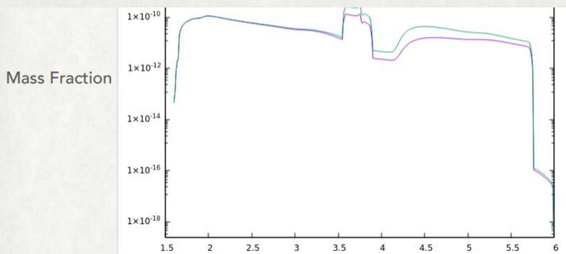


Group Meeting July 8th 2022

## Current calculation

tegrated r

$$\left(\frac{N_{^{10}\mathrm{Be}}}{N_{^{9}\mathrm{Be}}}\right)_{ESS} \sim f\,\frac{(X_{^{10}\mathrm{Be}})_{SN}}{(X_{^{9}\mathrm{Be}})_{\odot} + (X_{^{9}\mathrm{Be}})_{SN}} \exp\left(\frac{-\Delta}{2\ \mathrm{Myr}}\right)$$

t~50s

| $(M_{\odot})$ | Be10 | Be9 | Be9 (solar mass fraction) |
|---|---|---|---|
| NH | 1.572E-10 | 8.181E-11 | 1.51E-10 |
| IH | 2.185E-10 | 1.060E-10 | 1.51E-10 |

T. Hayakawa et al. Astrophysical Journal Letters, 779, (2013)

1) $f \sim 1 \times 10^{-4}$ and $\Delta \sim 1$ Myr

2) $f \sim 3 \times 10^{-3}$ and $\Delta \sim 1$ Myr

Nature Communications, (2016), 7

3) $f \sim 5 \times 10^{-4}$ and $\Delta \sim 1$ Myr

**Table 1 | Yields of short-lived radionuclides from an 11.8-solar-mass core-collapse supernova.**

| R/I | $\tau_R$ (Myr) | $Y_R$ ($M_{\odot}$) | $X_I^{\odot}$ | $(N_R/N_I)_{ESS}$ Data | Case 1 | Case 2 | Case 3 |
|---|---|---|---|---|---|---|---|
| $^{10}$Be/$^{9}$Be | 2.00 | 3.26(−10) | 1.40(−10) | (7.5±2.5)(−4) | 6.35(−4) | 6.35(−4) | 5.20(−4) |

$$(7.5 \pm 2.5) \times 10^{-4} \sim f\,\frac{(X_{^{10}\mathrm{Be}})_{SN}}{(X_{^{9}\mathrm{Be}})_{\odot} + (X_{^{9}\mathrm{Be}})_{SN}} \exp\left(\frac{-\Delta}{2\ \mathrm{Myr}}\right)$$

| Parameter set | 1) | 2) | 3) | meteorite |
|---|---|---|---|---|
| NH | 4.551E-05 | 1.365E-03 | 2.275E-04 | 5E-4 ~ 1E-3 |
| IH | 5.730E-05 | 1.719E-03 | 2.865E-04 | |

**Summary 1**
**As suggested by Nature, we used new data for 10Be(a,n)13C from JINA REACLIB .**
**But 10Be abundance is very small.**

**Summary 2**
**Previous calculation used the Talys results for 10Be(p,n)10B, which destroyed 10Be.**
**But new calculations based on JENDL-5 showed that the (p,n) reaction is small,**
**so that**
**10Be abundance increases.**

The CEX is really important and needs the experimental data !!

# Nuclear reaction around 10Be

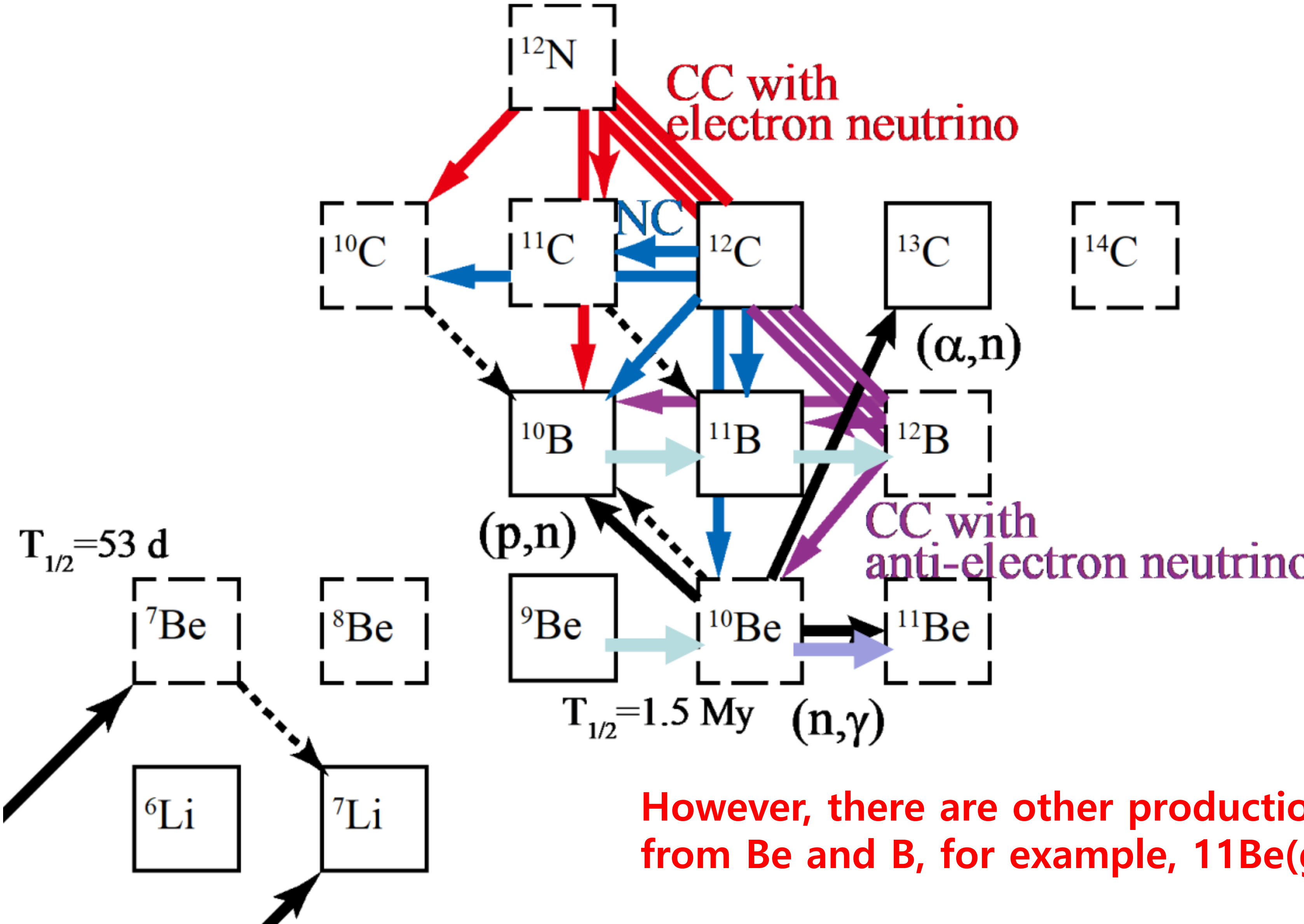


**However, there are other production channels from Be and B, for example, 11Be(g,n)10Be....**

The role of low-lying resonances for the $^{10}Be(p, \alpha)^{7}Li$ reaction rate and implications for the formation of the Solar System

A. Sieverding,[1,*] J. S. Randhawa,[2] D. Zetterberg,[1,3] R. J. deBoer,[2]
T. Ahn,[2] R. Mancino,[4,5] G. Martínez-Pinedo,[5,4] and W. R. Hix[1,3]

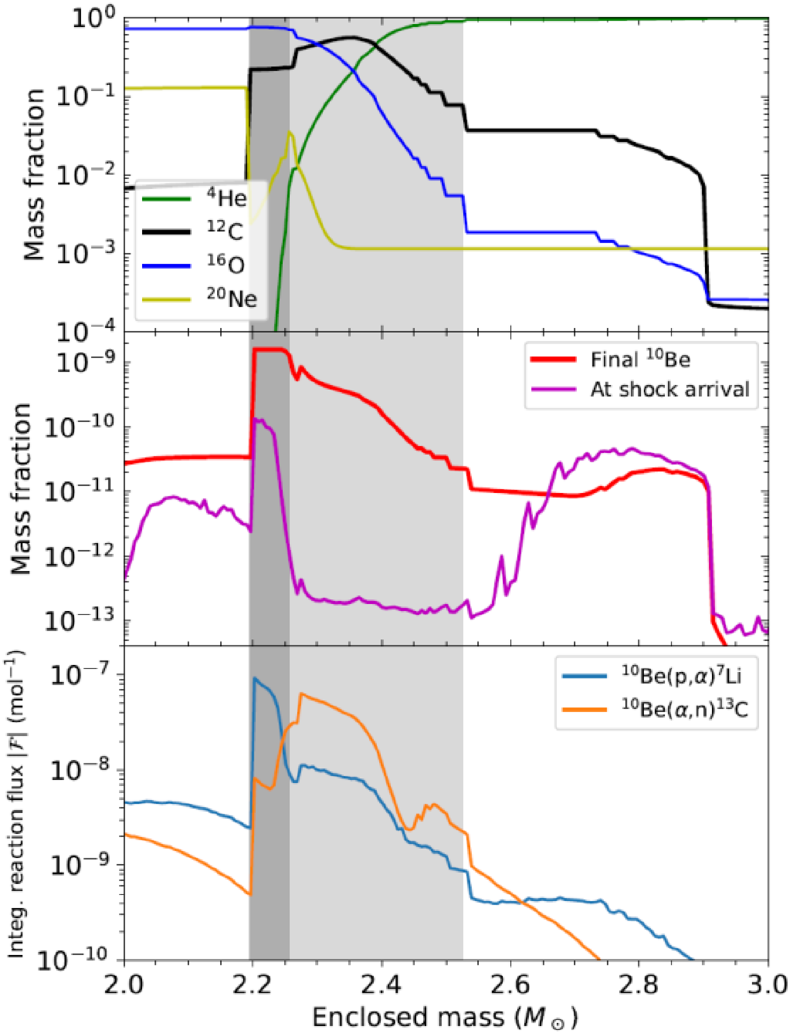


Phys. Rev. C **106**, 015803, 2022

It is pointed out that the dominant destruction channel is 10Be(p, alpha)7Li reaction.

They calculated the cross section taking the resonances on 11B into account.


Why $^{11}Be(\gamma,n)^{10}Be$ is so high?
$^{11}$Be은 주로 $^{12}C+\bar{\nu}_e$로 부터 생기긴 함
$M_r$ = 2.00 $M_\odot$
$M_r$ = 2.63 $M_\odot$
$M_r$ = 3.74 $M_\odot$
$M_r$ = 3.25 $M_\odot$
$M_r$ = 3.98 $M_\odot$
$M_r$ = 4.93 $M_\odot$
integrate dY/dt over t
reactions
$^{11}Li(weak)^{11}Be$
$^{11}Be(weak)^{11}B$
$^{11}Be(\gamma,n)^{10}Be$
$^{11}Be(\gamma,\alpha)^{7}Li$
$^{12}Be(\gamma,n)^{11}Be$
$^{10}Be(n,\gamma)^{11}Be$
$^{11}Be(n,\gamma)^{12}Be$
$^{8}Li(\alpha,p)^{11}Be$
$^{11}Be(p,\alpha)^{8}Li$
$^{11}Be(\alpha,n)^{14}C$
$^{14}C(n,\alpha)^{11}Be$
$^{12}C+\bar{\nu}_e$ $^{11}Be$
Group Meeting July 8th 2022

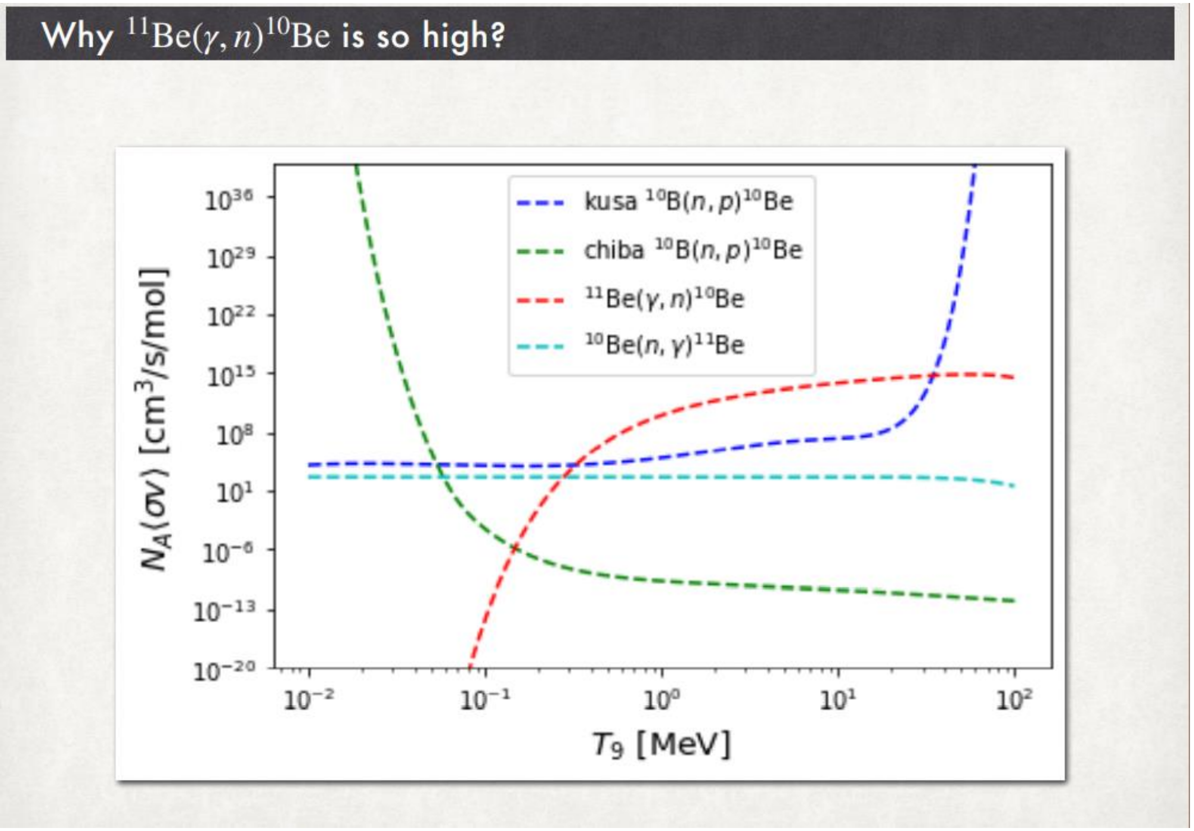


We used the (n,g) data from NNDC and calculated reverse reaction by the balance equation.
The contribution turns out to be critical for the 10Be production process.
Of course, we need experimental data to justify these reactions.

# Contents

- **Sterile Neutrinos & Shock Effects in Neutrino Process**
- **Summary**

# Neutrino process | Summary

- Neutrino spectra are largely changed by the neutrino self-interaction for inverted mass hierarchy case.
- Heavy elements, $^{92}$Nb, $^{138}$La $^{98}$Tc and $^{180}$Ta, are mainly produced in inner region below O-Ne-Mg layer, and increased about 3 or 4 times larger by the neutrino self-interaction. But, $^{180}$Ta abundance depends on the pre-supernova model.
- Although there is shock propagation, MSW effect impacts rarely on heavy elements. (But with other hydrodynamics model it can affect them.)
- All results hinge on the luminosity. For example, if we take some numerical luminosities **from the simulation of the neutrino transportation, results show that the situation is reversed**.
- Light elements, which are produced in outer region, turn out to be mainly sensitive on the MSW effects.
- Mass hierarchy can be determined by more accurate data of 7Li/11B ratio in the astronomy.
- **Ratio of 138La/11B could be an interesting quantity for SI and MSW effects. It favors the Normal Hierarchy !!!**
- Sterile neutrinos are allowed in the equivalent luminosity scenario with **NH scheme.**

Thanks
for
your
attention !

OMEG
Origin of Matter and Evolution of Galaxies
Key Research Institutes in Universities

# for Multi-messenger Nuclear Astrophysics

## Member of OMEG (Origin of Matter and Evolution of Galaxies)

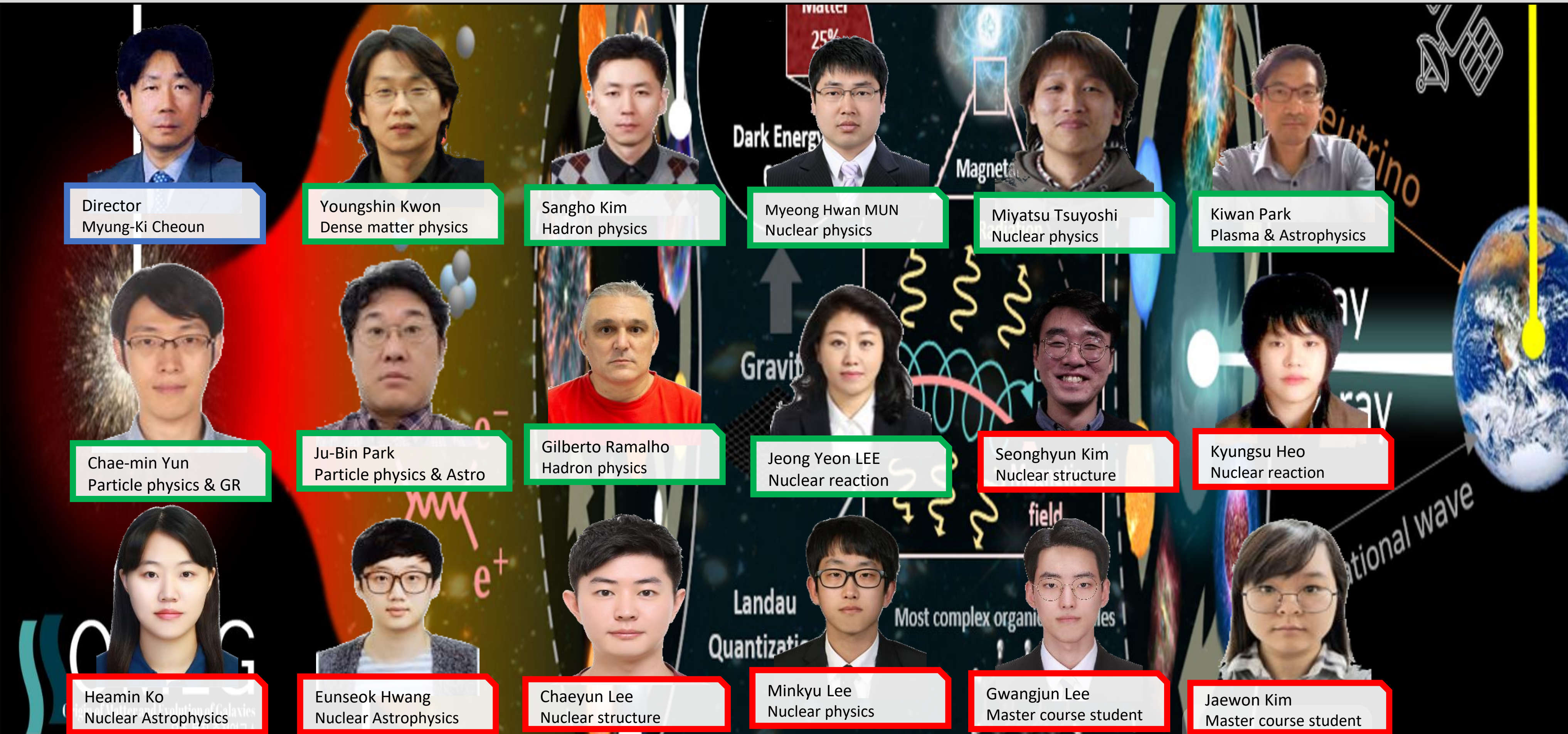


Collaboration : AMoRE, JSNS^2, DRHBc Mass Model, CENS

Colleagues : Kyungsik Kim, K. Choi (KAU), Eunja Ha (Hanyang), W. Y. SO(Kangwon), C. Hyun (Daegu)...

T. Kajino, M. Kusakabe (Beihang), B. Balantekin (Wisconsin), G. Mathews (Nortre Dame),

T. Maruyama (Nihon), H. Sagawa (RIKEN), K. Hagino(Kyoto), E. Hiyama (Tohoku), T. Kawano (BNL)....

**Recruitment : We are looking for researchers to join this project !!! Achieve Your Dreams With**